JOURNAL OF CHEMOMETRICS, VOL. 11, 419–461 (1997)

ANALYTICAL FIGURES OF MERIT FOR TENSORIAL CALIBRATION

KLAAS FABER,[1]* AVRAHAM LORBER[2] AND BRUCE R. KOWALSKI[1]**
[1] *Center for Process Analytical Chemistry, University of Washington, Box 351700, Seattle, WA 98195, U.S.A.*
[2] *Nuclear Research Centre-Negev, PO Box 9001, Beer-Sheva 84190, Israel*

SUMMARY

The subject of analytical figures of merit for tensorial calibration is critically reviewed. Tensorial calibration derives its name from tensor algebra, which provides a classification of calibration methods depending on the complexity of the data obtained for one chemical sample. Expressions for net analyte signal, sensitivity (classical model formulation), 'inverse sensitivity' (inverse model formulation), selectivity, signal-to-noise ratio and limit of detection (in signal space) are proposed for *N*th-order data ($N \geqslant 2$) that are consistent with the accepted zeroth-order definitions and previously proposed definitions for first-order data. Useful relationships between the proposed figures of merit and prediction error variance are described. A selectivity-based rule of thumb is derived to compare data analysis across orders. Central to the currently proposed framework for analytical figures of merit is the reduction of a complex data structure to the scalar net analyte signal. This allows for the construction of a univariate calibration graph (classical or inverse model), independent of the complexity of the data. Enhanced visualization and interpretation are obtained that may help to bridge the gap between *N*th-order calibration and the intuitive understanding of zeroth-order data. © 1997 John Wiley & Sons, Ltd.

Journal of Chemometrics, Vol. **11,** 419–461 (1997) (No. of Figures: 18 No. of Tables: 14 No. of References: 50)

KEY WORDS figures of merit; calibration

INTRODUCTION

Analytical figures of merit are performance characteristics of an analytical determination. They can be used to select between potentially useful methods or to evaluate or optimize a method that is already in use.[1] Analytical figures of merit are well-defined for univariate calibration where a single response (scalar) is measured for a chemical sample. Consider a linear calibration function that relates analyte concentration to net analyte signal (see Figure 1). The net analyte signal is obtained by a suitable background correction. An example of an analytical figure of merit is the sensitivity, which in this case is given by the slope of the calibration function. A high sensitivity is desirable, since this allows small changes in analyte concentration to be detected. A high sensitivity is therefore almost synonymous to a low detection limit and a small prediction error. Other figures of merit such as the signal-to-noise ratio and the selectivity have an equally straightforward and intuitive interpretation.

The situation is obviously more complicated if a more complex data structure is measured for a single chemical sample and accordingly more sophisticated calibration methods are used to predict analyte concentrations. Following the tensorial terminology introduced by Sánchez and Kowalski[2, 3] into the field of calibration, a scalar is a zeroth-order tensor, a vector is a first-order tensor and a matrix with a certain structure is a second-order tensor. This paper will only be concerned with matrices that have a bilinear structure. This does not severely restrict the applicability of the associated figures of

* Current address: Netherlands Forensic Science Institute, Volmerlaan 17, NL-2288 GD Rijswijk, Netherlands
** Correspondence to: B. R. Kowalski

CCC 0886–9383/97/050419–43 $17.50

Received 15 November 1996
Accepted 27 March 1997

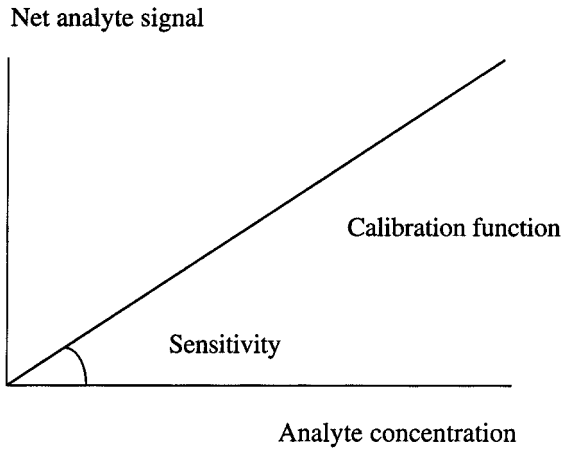

Figure 1. Relationship between net analyte signal, analyte concentration and sensitivity for a linear calibration function under the classical model

merit, since the bilinear model is often suited for the analysis of chemical data. The reason for this is that this model is consistent with physicochemical laws such as the Beer–Lambert law in spectroscopy. For example, instruments of the 'hyphenated' type such as a chromatograph coupled with a multichannel detector give bilinear data, since the chromatography can be assumed to be independent of the spectroscopy and *vice versa*. This ensures a bilinear structure of the resulting response matrix. For higher-order tensors the multilinear model is assumed for which the same considerations with respect to applicability hold.

Although calibration using scalars, vectors and matrices (and beyond) has been satisfactorily unified, this is not yet the case for their associated analytical figures of merit. A framework for figures of merit for first-order data has been introduced by Lorber.[4,5] This framework was originally developed within the *classical model* where the instrumental response is modeled as a function of analyte concentration (see Figure 1). Very recently, significant advances have been made with respect to the calculation of figures of merit in the *inverse model* where the analyte concentration is modeled as a function of instrumental response. [6] The inverse model is the preferred model in practice, since it is less restrictive; the classical model can be applied if the concentrations of all interferents are known. This usually not achievable in, for example, environmental work or applications in the food industry. Of pivotal importance to Lorber's framework is the definition of net analyte signal as *the part of the gross signal that is useful for calibration*. Principles gleaned from linear algebra led to the mathematical requirement that the net analyte signal vector of the analyte be orthogonal to the signal vectors of the interferents. Using the net analyte signal calculated in this way, the other figures of merit were derived in a straightforward fashion. In this paper we will restrict ourselves to the calculation of the sensitivity, selectivity, signal-to-noise ratio and limit of detection. The useful relationship between Lorber's figures of merit and prediction error variance has been pointed out by Bauer *et al.* [7]

Lorber's framework is, however, not without controversy. Very recently, Kalivas and Lang[8] criticized Lorber's definition of sensitivity for containing selectivity information. Selectivity measures the amount of overlap between the response of the analyte and the response of the interferents. According to Kalivas and Lang, the sensitivity should not depend on the signal of the interferents and they consequently propose the definition of first-order sensitivity introduced by Bergmann *et al*.[9] This definition amounts to calculating the Euclidean norm of the vector of partial sensitivies associated with the analyte of interest. This definition will generally give different numerical values. Identical

results will only be obtained if the data are fully selective for the analyte of interest, i.e. there is no overlap with the interferents, which, however, may be overlapped among themselves. Thus generally accepted definitions for the analytical figures of merit do not exist for first-order data. Neither have recommendations been issued by regulatory bodies such as the International Union of Pure and Applied Chemistry (IUPAC) to the authors' knowledge.

An equally disturbing controversial situation is found in the chemometrics literature that is concerned with defining analytical figures of merit for second-order calibration. The second-order analogue for Lorber's first-order selectivity has been published by Ho *et al*.[10] and was extended by Appellof and Davidson[11] to third-order data. They used the term *uniqueness* to indicate the amount of the analyte response matrix that is unique to the sought-for component, i.e. the part of the analyte response matrix that is free from overlap. The uniqueness concept was developed to improve the reliability of the analysis of bilinear data using the method of rank annihilation factor analysis (RAFA). Ho *et al*. showed how prediction error variance related to uniqueness. Their error analysis, however, only takes the uncertainty in part of the data into account. Their expression for prediction error variance has recently been improved by Faber *et al*.[12] The relationship between uniqueness and prediction error variance demonstrates the utility of the uniqueness concept. The equivalence between uniqueness and selectivity has been mentioned by Lorber and Kowalski.[13] Although it seems certain that Ho *et al*. have prepared the ground for defining analytical figures of merit for second-order calibration, the extension of Lorber's framework along this line has not yet been carried out to the authors' knowledge. One reason may be that the work of Ho *et al*. was considered to be obsolete when the (non-iterative) generalized rank annihilation method (GRAM) replaced the somewhat cumbersome iterative RAFA technique.[14] Another reason could be the skepticism with which the uniqueness was originally introduced. Ho *et al*. already pointed out that to calculate the uniqueness pure component response matrices are necessary and this information is generally not available. However, as discovered later, using GRAM, full curve resolution can be obtained and the uniqueness is easily computed. It is worth mentioning that Wilson and Kowalski[15] defined the net analyte signal consistent with the uniqueness. They used the net analyte signal to develop a curve resolution method ('net analyte signal maximization'), but the results were poor and this work has not been continued. Sánchez and Kowalski[3] identified the contravariant vectors for the individual modes of a second-order tensor but did not translate this information into a definition of net analyte signal. Wang *et al*.[16] introduced a definition of net analyte signal that is based on the following consideration. With second-order bilinear data, quantitation can be achieved in the presence of unknown interferents using *one* calibration sample only. This is the so-called second-order advantage. A logical step is then to assume that the entire signal is used for calibration and the net signal was defined accordingly, i.e. the net signal was assumed to be identical to the gross signal. This work has recently been reviewed in the larger context of tensorial calibration by Booksh and Kowalski.[17] It is noted that their definition is not based on the use of a projection matrix and is therefore consistent with the definition of first-order sensitivity proposed by Bergmann *et al*.[9] Finally, very recently, Messick *et al*.[18] have proposed to calculate the net signal analogous to Lorber's first-order net signal. However, the projection matrix they derive is different from the projection matrix that leads to the uniqueness.

From the literature survey given above, it is clear that the situation for second-order figures of merit is even more controversial than for their first-order counterparts. There is, however, an important similarity. For both first- and second-order data it has been proposed to use a projection to remove the contribution of the interferents. The only difference is that for second-order data, several projections have been proposed. Contrasting these definitions are the attempts to define net analyte signal without a projection. The presence of many competing and mutually excluding definitions is the motivation for the current work. The purpose of this paper is to revisit expressions presented in the chemometrics literature and arrive at a coherent framework for zeroth-, first- and second-order calibration (and

beyond). The foundation has been laid a long time ago[4, 10] and the new expressions presented here should be self-explaining. The goal of the current work is to help bridge the gap between *N*th-order calibration and the intuitive understanding of zeroth-order data. A framework of analytical figures of merit for *N*th-order calibration can only be expected to be successful in this respect if the interpretability of zeroth-order calibration is maintained. Of paramount importance is that the complexity of the response data remains invisible to the end user. Thus a presentation of the model as a simple univariate calibration graph with 'pseudo-zeroth-order'analytical figures of merit is pursued.

In this paper, focus will be on the figures of merit that only depend on the data. Prediction error variance, for example, depends on the estimation method used and can therefore not be considered as an analytical figure of merit unless the estimation method is seen as an integral part of the analytical method. This is a matter of dispute and addressing this point is considered to be outside the scope of this paper. These considerations are relevant in, for example, first-order calibration where ordinary least squares (OLS), principal component regression (PCR) and partial least squares (PLS) are popular methods. The same holds for second-order calibration where the choice is between GRAM (and variations thereof) and alternating least squares (ALS) methods.

Potential applications of this work obviously include method selection, evaluation and optimization but also improved interpretation of the data analysis as pointed out by Messick *et al*. with respect to the results of a curve resolution study of Grung and Kvalheim.[19] A successful first-order method optimization using net analyte signal is very recently reported by Xu and Schechter.[20] In their work the optimal wavelength region in severely overlapped fluorescence spectra was selected. Wavelength selection (or more general variable selection) is certainly an issue in second-order data analysis (and beyond), since now two sets of variables (or more) have to be scrutinized for their suitability. Another field where analytical figures of merit may be useful is data pretreatment. Data pretreatment alters the quality of the data and this may be reflected in the numerical values for the figures of merit. Conversely, the analytical figures of merit could be used to drive the data pretreatment.

THEORY

The plethora of definitions for second-order net analyte signal and analytical figures of merit illustrates that a proper definition can hardly be formulated without considering the context within which it should work. The context in this paper is calibration and in this section calibration will therefore be treated in sufficient detail to make the currently proposed framework for analytical figures of merit transparent to a potential user. Well-known expressions for zeroth-order and first-order calibration are reviewed to show that a natural progression is possible from zeroth-order via first-order to second-order and beyond.

Notation

Scalars are denoted by italics, e.g. a. Boldface letters are used for column vectors (lowercase) and matrices (uppercase), e.g. $\mathbf{a}$ and $\mathbf{A}$. Underlined boldface uppercase letters are used to denote Nth-order tensors ($N \geqslant 2$), e.g. $\underline{\mathbf{A}}$. Matrices with bilinear structure are second-order tensors. In expressions that generally hold for Nth-order tensors, matrices will follow the notation for tensors. In special cases ($N=2$) the notation for matrices is used for simplification. Transposition of a vector or matrix is symbolized by the superscript 'T', e.g. $\mathbf{A}^{\mathrm{T}}$ and $\mathbf{a}^{\mathrm{T}}$. The inverse and Moore–Penrose pseudoinverse of a matrix $\mathbf{A}$ are denoted by $\mathbf{A}^{-1}$ and $\mathbf{A}^{+}$ respectively. The 'inverse transpose' and 'pseudoinverse transpose' are symbolized by $\mathbf{A}^{-\mathrm{T}}=(\mathbf{A}^{-1})^{\mathrm{T}}=(\mathbf{A}^{\mathrm{T}})^{-1}$ and $\mathbf{A}^{+\mathrm{T}}=(\mathbf{A}^{+})^{\mathrm{T}}=(\mathbf{A}^{\mathrm{T}})^{+}$ respectively. Measured and estimated (or predicted) quantities are symbolized by adding a 'tilde' or a 'hat' to the symbol of the true quantity, e.g. $\tilde{\mathbf{A}}$ and $\hat{\mathbf{A}}$.

Terminology

Without loss of generality it is assumed in this paper that a model is built to predict analyte concentrations from measured instrumental responses. This leads to a fair amount of chemical terminology. Most attention will be paid to the classical model, but connections with the inverse model are occasionally made. The statistical terms 'object' (or 'observation'), 'variable', 'predictor' (or 'regressor') and 'predictand' (or 'response variable') are replaced by 'chemical sample', 'wavelength' (or 'channel'), 'instrumental response' and 'analyte concentration' respectively. This determines the dimension of the analytical figures of merit. For example, the sensitivity in the classical model will have unit response/concentration. In the inverse model the role of analyte concentration and instrumental response is reversed, which leads, for example, to an 'inverse sensitivity' with unit concentration/response.

In statistics a clear distinction is made between estimation, which pertains to a *parameter* (a constant), and prediction, which pertains to a *random variable*. In the current context, for example, the sensitivity is a model parameter but the net analyte signal is a random variable. Generally, unknown quantities that depend on the chemical sample under scrutiny are random variables which are predicted rather than estimated. In analytical chemistry this distinction is usually not made and we will loosely use estimation and prediction as interchangeable terms. This will not affect any of the results presented here.

The key concept in this paper is net analyte signal (or response). Confusion has arisen in the past because this term is simultaneously used to denote the net contribution of the analyte to the gross response vector in first-order calibration as well as the Euclidean norm of that 'net response vector'. At places where confusion might arise, the term 'net partial responses' will be used to differentiate between the vector and its norm. The same terminology is proposed for second-order data (and beyond). It is consistent with the term 'partial sensitivity' which is defined as the sensitivity of the instrumental response at a particular wavelength for a change in analyte concentration.[9] Consistent with 'net partial response', the term 'net partial sensivity' is proposed to denote the part of the partial sensitivity which is free from overlap of interferents.

Analytical figures of merit for zeroth-order calibration

Here and in the following sections the errors are dropped from the equations for simplifying reasons. This leads to definitions of analytical figures of merit in terms of errorless quantities, which have to be replaced in practice by measured or estimated (predicted) values.

Consider a linear model between background-corrected signal and concentration. The background correction leads to a zero-intercept model. In the calibration step, responses are measured for I samples with known concentrations. The resulting data can be arranged as

$$\mathbf{r}_0^* = \mathbf{r}_0 - \mathbf{b}_0 = s\mathbf{c}_0 \tag{1}$$

where $\mathbf{r}_0^*$ ($I \times 1$) denotes the net signal vector, $\mathbf{r}_0$ ($I \times 1$) is the gross signal vector, $\mathbf{b}_0$ ($I \times 1$) is the background vector, s denotes the sensitivity and $\mathbf{c}_0$ ($I \times 1$) is the vector of known concentrations. The subscript '0' indicates that the quantities belong to the calibration step. Background correction of the gross signal leads to the net signal. A successful background correction in zeroth-order calibration eliminates the contribution of *all* (spectrally active) interferents. This is necessary since the model cannot accommodate for interferents and an incomplete background correction eventually leads to biased concentration estimates.

The model for the prediction sample data is

$$r^* = r - b = sc \tag{2}$$

where r^* is the net signal, r is the gross signal, b is the background and c is the unknown concentration to be determined. Having identified the net signal, it is straightforward to derive the figures of merit. In the following, focus will be on the prediction sample, since figures of merit may be sample-dependent (e.g. the signal-to-noise ratio) and prediction is the ultimate goal of the calibration.

The sensitivity, defined as the slope of the calibration line, is given as

$$s = r^*/c \tag{3}$$

The relation with the slope ('inverse sensitivity') found in the inverse model, $c = \beta r^*$, is

$$s = \beta^{-1} \tag{4}$$

The selectivity is defined as the ratio of the net and the gross signal:

$$\xi = r^*/r \tag{5}$$

The selectivity quantifies the loss of signal due to interferents and ranges between zero (no selectivity) and one (full selectivity). Other definitions exist which are often specific for a certain application area (e.g. ion-selective electrodes in electrochemistry), but the definition given above anticipates the definition for first-order data given in the next section. The fact that the latter definition is now widely accepted justifies the current definition of zeroth-order selectivity within the context of this paper.

The signal-to-noise ratio (S/N) is defined as

$$\rho = r^*/\sigma(\tilde{r}^*) = r^*/\sigma_{r-b} \tag{6}$$

where $\sigma_{r-b} = \sqrt{(\sigma_r^2 + \sigma_b^2)}$ is the standard deviation of the measurement noise in the background-corrected signal. This expression shows that one has to pay a price for the background correction in the form of an increased response error. It is noted that often the background-corrected signal obtained from an actual measurement is denoted as the *estimated* net analyte signal, i.e. $\hat{r}^*$ in the current notation (more precisely, *predicted* net analyte signal). Here the notation $\tilde{r}^*$ is preferred because the background correction is usually performed by the instrument, i.e. the net analyte signal is *measured* and not obtained by an operation on the data produced by the instrument.

Finally, the definition for the limit of detection (LOD) recommended by IUPAC is given by[21]

$$L_D = k_\alpha \cdot \sigma(\tilde{r}^* \mid H_O) + k_\beta \cdot \sigma(\tilde{r}^* \mid H_A) \approx (k_\alpha + k_\beta) \cdot \sigma_{r-b} \tag{7}$$

where $\sigma(\tilde{r}^* \mid H_O)$ and $\sigma(\tilde{r}^* \mid H_A)$ are the measurement uncertainties in the net signal under the null hypothesis H_O (no analyte present) and the alternative hypothesis H_A (analyte present at level of detection limit) and k_α and k_β are multipliers that lead to a certain error of the first kind (false positive), α, and second kind (false negative), β.* According to equation (7), one needs to know the measurement uncertainty in the background-corrected signal at certain specific levels of the analyte. The far right-hand side is the simplification that results from assuming a measurement uncertainty that is independent of the signal. Accepting an error rate of 7% for both α and β and assuming a normal distribution for the response error leads to the useful rule of thumb that the limit of detection is the response that gives a signal-to-noise ratio of three. Figure 2 illustrates the concepts of limit of detection and limit of decision. Note that in this schematic representation the width of the distributions is a function of the size of the net signal. Depending on the application at hand, the simplification of equation (7) may be acceptable or not in this specific example.

The limit of detection is the *a priori* value (i.e. before the actual measurement is made) that the net

* The symbol for the error of the second kind (β) is also in use for the 'inverse sensitivity'. The meaning should be clear from the context.

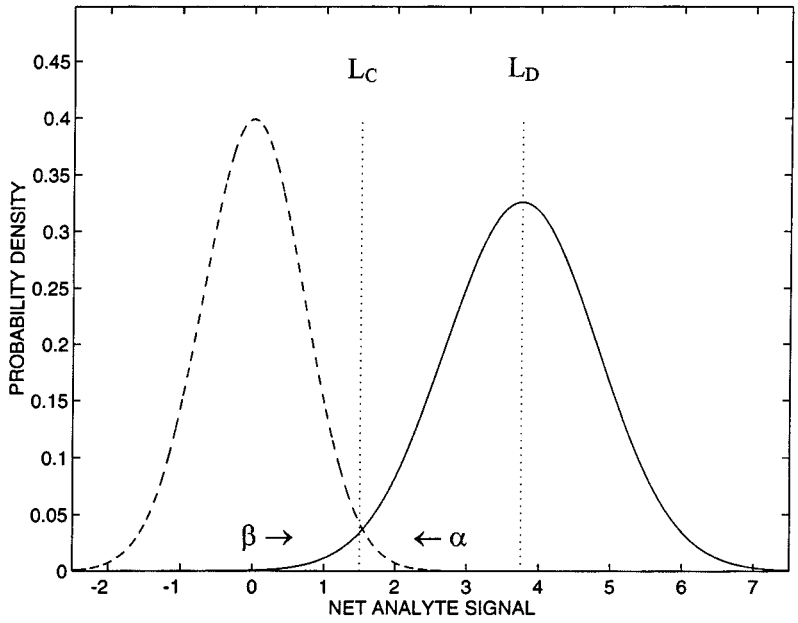

Figure 2. Illustration of limit of decision (L_C) and limit of detection (L_D) as recommended by IUPAC. The limit of decision is only determined by the distribution under the null hypothesis H_O (broken line). In contrast, the limit of detection is also determined by the distribution under the alternative hypothesis H_A (full line)

response must exceed to enable detection of the analyte. The limit of decision, which is lower than the limit of detection, is the *a posteriori* value (i.e. after the actual measurement is made) that the net response must exceed to enable detection of the analyte. The definition of limit of detection given above has proved to be difficult to understand for analytical chemists. Especially the need for two limiting values (decision and detection limit) is a continuing source of misunderstanding. However, the introduction of two limiting values really makes sense from a decision science point of view, because the measurement itself increases the information that can be used to solve the analytical detection problem (for further discussion see Reference 1).

The subject of detection limit will be approached in a somewhat qualitative fashion in the remainder of this paper, since it merits a separate treatment. In the discussion of the limit of detection for first- and second-order data the emphasis will be on pointing out an important difference with equation (7). Other limiting values for the net signal such as the limit of guarantee of purity, limit of quantitation and limit of determination, which only differ with respect to the size of the expected errors of the first and second kind,[22] are obtained analogously.

Finally, in the above discussion the limit of detection has been defined in response space. The possiblity of defining the limit of detection in terms of the uncertainty in the predicted concentration rather than the uncertainty in the net response has already been pointed out by Long and Winefordner.[23] The expressions for prediction error variance given below could offer a starting point for the calculation for zeroth-, first- and second-order data. In this work we have chosen to work in response space, since defining the limit of detection in concentration space makes it a function of the estimation method.

Emphasis in the next sections should be on obtaining expressions that allow for a straightforward comparison with the expressions well-known and well-understood for the zeroth-order case, i.e. equations (3)–(7).

Analytical figures of merit for first-order calibration

Going from zeroth-order to first-order data allows for quantitation in the presence of interferents. This is the so-called first-order advantage. A logical consequence of going to first-order data is that the figures of merit will no longer be characteristic for the analytical procedure. Instead they will be characteristic for the analyte of interest. In addition, some of the figures of merit will be sample-specific like the signal-to-noise ratio in the zeroth-order case. This increased complexity will certainly tend to impede their use in analytical practice unless expressions can be derived that are natural analogues of their zeroth-order counterparts.

Consider a linear model between background-corrected responses and concentrations. If the responses for K components are obtained at J wavelengths by measuring I calibration samples, the data can be represented as

$$\mathbf{R}_0^{\mathrm{T}} - \mathbf{B}_0^{\mathrm{T}} = \mathbf{S}\mathbf{C}_0^{\mathrm{T}} \tag{8}$$

where $\mathbf{R}_0$ ($I \times J$) is the gross response matrix, $\mathbf{B}_0$ ($I \times J$) is the background matrix, $\mathbf{S}$ ($J \times K$) is the matrix of 'partial' sensitivies (or calibration constants) and $\mathbf{C}_0$ ($I \times K$) is the matrix with known concentrations. It is emphasized that in many applications a background correction may not be necessary. However, including the background correction in the equations leads to a general treatment.

The model for the prediction sample data is

$$\mathbf{r} - \mathbf{b} = \mathbf{S}\mathbf{c} \tag{9}$$

where $\mathbf{r}$ ($J \times 1$) is the gross response vector, $\mathbf{b}$ ($J \times 1$) is the background vector and $\mathbf{c}$ ($K \times 1$) is the concentration vector to be predicted. The background correction is necessary to remove sources of variation that cannot be modeled but does not lead to a net analyte signal as in the zeroth-order case. The reason for this is that multiple components (K) are modeled and the overlap between these components reduces the part of the signal that can be used for quantitation.

Lorber[4] argued that the net analyte signal is the *part of the signal that is unique to the analyte of interest*. (In the remainder of the paper the analyte of interest will be denoted by the index k). The unique part is obtained by applying an orthogonal projection matrix to the background-corrected unknown sample response vector:

$$\mathbf{r}_k^* = (\mathbf{I}_J - \mathbf{S}_{-k}\mathbf{S}_{-k}^{+})(\mathbf{r} - \mathbf{b}) = \mathbf{P}_{k,\mathbf{S}}(\mathbf{r} - \mathbf{b}) \tag{10}$$

where $\mathbf{r}_k^*$ ($J \times 1$) is the net contribution of the kth analyte to $\mathbf{r} - \mathbf{b}$, $\mathbf{I}_J$ ($J \times J$) is the identity matrix and $\mathbf{S}_{-k}$ ($J \times (K-1)$) is the matrix $\mathbf{S}$ without the kth column. This projection process is illustrated geometrically in Figure 3. It follows that in an experimental situation one obtains an estimate (or prediction) of the true net analyte signal, denoted by $\hat{r}^*$, rather than $\tilde{r}^*$ as in the zeroth-order case.

The 'net partial sensitivities' are obtained as

$$\mathbf{s}_k^* = \mathbf{r}_k^* / c_k \tag{11}$$

where c_k is the kth component of $\mathbf{c}$.

The net analyte signal is calculated as the Euclidean norm of the vector of the 'net partial responses':

$$r_k^* = \| \mathbf{r}_k^* \| \tag{12}$$

The sensitivity is defined by

$$s_k = \| \mathbf{s}_k^* \| = r_k^* / c_k \tag{13}$$

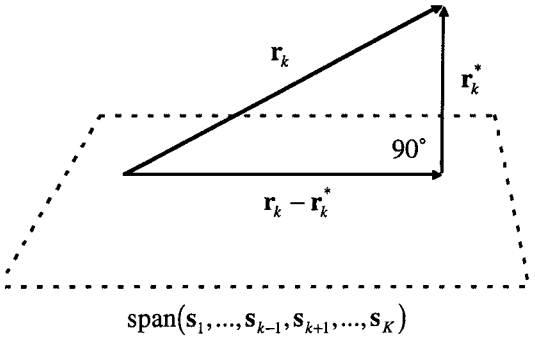

Figure 3. Geometrical representation of first-order net analyte signal. The net analyte signal vector $\mathbf{r}_k^*$ is orthogonal to the space spanned by the $K-1$ columns of $\mathbf{S}$ that are associated with the interferents (i.e. $\mathbf{s}_{k'}$ with $k' \neq k$)

It is important to note that the choice for the Euclidean norm in equations (12) and (13) is not trivial. Kalivas and Lang[8] discuss the possibility of using other vector norms to convert a vector into a scalar value. However, only the use of the Euclidean norm will enable the derivation of simple expressions of prediction error variance in terms of the sensitivity defined by equation (13) and is therefore the natural choice (see below). The relation with the regression vector $\boldsymbol{\beta}_k$ found in the inverse model is[13]

$$s_k = \beta_k^{-1} = \| \boldsymbol{\beta}_k \|^{-1} \tag{14}$$

where β_k is the extension of the 'inverse sensitivity' to first-order data. In tensorial language the regression vector is the *contravariant* vector.[2] It is noted that this simple relation (cf. equation (4)) is only possible if the sensitivity is defined as in equation (13). Kalivas and Lang[8] argue that Lorber's definition is not accurate, since it includes selectivity information (through the net analyte signal), and instead prefer the definition of Bergmann *et al*.[9] According to this definition, the sensitivity is calculated as the Euclidean norm of the vector of partial sensitivities rather than the net contribution. It therefore does not include selectivity information, which is due to interferents and not to the analyte. This definition is also well-motivated. However, it will lead to more complex expressions than obtainable using Lorber's definition (13). In addition, it is worth noting that traditionally the regression vector in the inverse model is allowed to include the overlap with the interferents. Finally, in the univariate classical model the sensitivity is calculated from a net analyte signal that also includes selectivity information. These arguments taken together lead to a definition of sensitivity that includes selectivity information. Although counter-intuitive to some extent, it leads to a coherent framework of figures of merit. In addition, simple relationships with prediction error variance can be established in this way (see below). Being able to express prediction error variance in analytical chemical terms is an added bonus that cannot be underestimated.

The selectivity measures the amount of overlap with the modeled interferents:

$$\xi_k = r_k^* / \| \mathbf{r}_k \| \tag{15}$$

where $\mathbf{r}_k = c_k \mathbf{s}_k$ and $\mathbf{s}_k$ is the kth column of $\mathbf{S}$. It is noted that very recently a method for the calculation of net analyte signal in the inverse model has been proposed.[6] This does not yet, however, enable the calculation of selectivity according to equation (15), since the pure component spectrum $\mathbf{s}_k$ is needed. Instead a sample-specific selectivity was defined by $\xi_k = r_k^* / \| \mathbf{r} \|$. This expression will always lead to smaller selectivity values than equation (15), unless there are no interferents ($\| \mathbf{r} \| = \| \sum \mathbf{r}_k \| \geqslant \| \mathbf{r}_k \|$). Owing to this sample dependence, the later definition may be more meaningful, but this remains a subject for further study. Otto and Wegscheider[24] and Kalivas and Lang[25] have reviewed alternative definitions of first-order selectivity.

The *approximate* signal-to-noise ratio is given by

$$\rho_k = r_k^* / \sigma(\hat{r}_k^*) \approx r_k^* / \sigma_{\mathbf{r}-\mathbf{b}} \tag{16}$$

where $\sigma_{\mathbf{r}-\mathbf{b}} = \sqrt{(\sigma_{\mathbf{r}}^2 + \sigma_{\mathbf{b}}^2)}$ is the standard deviation of the measurement noise in the background-corrected response vector. The denominator on the far right-hand side of equation (16) follows from performing error propagation on the estimated net analyte signal $\hat{r}_k^*$ and neglecting the uncertainty in estimating the projection matrix $\mathbf{P}_{k,\mathbf{S}} = \mathbf{I} - \mathbf{S}_{-k}\mathbf{S}_{-k}^{+}$ (see Appendix I). This approximation is justified, since in practice one only needs a rough estimate of the signal-to-noise ratio. In addition, this will make the results independent of the estimation method.

The *approximate* limit of detection in signal space is

$$L_{\mathrm{D},k} = E[\hat{r}_k^* \mid \mathrm{H_O}] + k_\alpha \cdot \sigma(\hat{r}_k^* \mid \mathrm{H_O}) + k_\beta \cdot \sigma(\hat{r}_k^* \mid \mathrm{H_A}) \approx E[\hat{r}_k^* \mid \mathrm{H_O}] + (k_\alpha + k_\beta) \cdot \sigma_{\mathbf{r}-\mathbf{b}} \tag{17}$$

where $E[\hat{r}_k^* \mid \mathrm{H_O}]$ is the expected value of the estimated net analyte signal under the null hypothesis, i.e. the analyte is absent, and the meaning of the remaining symbols is similar as explained under equation (7). This expression is different from its univariate analogue by the presence of the term $E[\hat{r}_k^* \mid \mathrm{H_O}]$, which is zero in the univariate case, since the instrumental errors can be assumed to have zero mean. However, the net analyte signal in the first-order case is calculated as the Euclidean norm of a vector and the Euclidean norm of a vector of zero-mean random variables is not zero. The reason for this is that the components of the vectors are squared before they are added. As a result the expected value will be a function of the variance of the individual components rather than their mean. This holds for the partial responses as well as for the net partial responses obtained by projection. The derivation of an approximate expression for the resulting *bias* is given in Appendix I. It is noted that this bias is identical for calibration and prediction samples alike. This bias will therefore be of no consequence if prediction is the goal of the data analysis, which it usually is. Using a biased model estimate will treat the calibration and prediction samples on an equal footing, which is correct. If, however, the goal is estimating the model, i.e. the true relationship between analyte concentration and net signal, then this bias has to be taken into account by subtracting it from the estimated net analyte signal. A numerical example of this bias correction will be given in a later section. A multivariate limit-of-detection estimator in concentration space was recently derived by Bauer *et al.*[26] and the subject of first-order limit of detection has very recently been reviewed by Boqué and Rius.[27]

Analytical figures of merit for second-order calibration

Going from first-order to second-order data enables quantitation in the presence of unknown interferents. This is the so-called second-order advantage, which is already achieved with only *one* calibration sample. Only the bilinear model will be considered here, since this will allow for a straightforward generalization of the expressions given in the previous sections. The extension to the 'non-bilinear' model as well as the generalization to multilinear models will be indicated in later sections. We will start off with the special case where only one calibration sample is available and return to the general case of multiple calibration samples at the end of this section.

It is important to note that with one calibration sample the model-building step and prediction step are different for second-order calibration than for their zeroth-order and first-order counterparts. In zeroth-order and first-order calibration a model is constructed using the responses and concentrations for the calibration samples. The model is then used to convert the prediction sample response(s) into a concentration estimate. In second-order calibration a 'model' is constructed from the responses of the calibration and prediction sample. This 'model' is then used to convert the calibration sample concentration into the desired concentration estimate for the prediction sample. Although the order of the operations is different for second-order calibration, the result is a concentration estimate. Thus for the analytical chemist who is going to apply the methodology (but is not interested in mathematical details) it should not make a difference whether the data analysis is zeroth-order, first-order or second-order. The primary task is to prepare samples, analyze them and report concentration estimates,

together with their uncertainty. The complexity of the response data should not make a difference to the analytical chemist during all these routine activities. The expressions for the figures of merit derived below and their relation to prediction error variance show that a framework can be developed where the complexity of the data only plays a superficial role, which is unimportant to the analytical chemist.

Consider the bilinear model leading to $J_1 \times J_2$ response matrices $\mathbf{R}$ and $\mathbf{R}_0$ for the prediction and calibration sample respectively.* The calibration sample can be a pure (one-component) sample or a mixture. Note that the format of these matrices is often variables $\times$ variables rather than objects (samples) $\times$ variables (wavelengths/sensors/channels) as in the first-order case. In the majority of current applications of second-order calibration techniques the data result from the combination of a chromatographic separation and multichannel detection. Prominent examples are liquid chromatography with ultraviolet detection (LC–UV) and gas chromatography combined with mass spectrometry (GC–MS). In these cases the variables in the first order are elution times and the variables in the second order are wavelengths or mass channels. Owing to the second-order advantage, no background correction is needed here; the background is treated as an unknown interferent.

In the simplest case the prediction sample contains all constituents present in the calibration sample. Considering this rather restricted case allows for deriving the net analyte signal and figures of merit in a straightforward way. Complications encountered in more general cases will be discussed later in this section and in sections that follow.

The model for the prediction sample response matrix is written as

$$\mathbf{R} = \sum_{k=1}^{K} \mathbf{R}_k = \sum_{k=1}^{K} \mathbf{x}_k \mathbf{y}_k^{\mathrm{T}} = \mathbf{X}\mathbf{Y}^{\mathrm{T}} \tag{18}$$

where $\mathbf{R}$ $(J_1 \times J_2)$ is the prediction sample response matrix, $\mathbf{R}_k$ $(J_1 \times J_2)$ is the kth analyte contribution to $\mathbf{R}$, $\mathbf{x}_k$ $(J_1 \times 1)$ is the kth column factor (e.g. an elution profile), $\mathbf{y}_k$ $(J_2 \times 1)$ is the kth row factor (e.g. a spectrum) and $\mathbf{X}$ and $\mathbf{Y}$ are the column and row factor matrices. The bilinear model derives its name from the fact that a response matrix, e.g. $\mathbf{R}$, can be expanded in bilinear terms. The data are linear in one order if the other order is kept fixed (conditional linearity). Thus in fact the bilinear model is nonlinear and this leads to estimation procedures which are different from the procedures used for analyzing zeroth-order and first-order data.

Equivalently, the calibration sample response matrix is given by

$$\mathbf{R}_0 = \sum_{k=1}^{K} \mathbf{R}_{k,0} = \sum_{k=1}^{K} \pi_k \mathbf{x}_k \mathbf{y}_k^{\mathrm{T}} = \mathbf{X}\boldsymbol{\Pi}\mathbf{Y}^{\mathrm{T}} \tag{19}$$

where $\mathbf{R}_0$ $(J_1 \times J_2)$ is the calibration sample response matrix, $\mathbf{R}_{k,0}$ $(J_1 \times J_2)$ is the kth analyte contribution to $\mathbf{R}_0$, $\pi_k = c_{k,0}/c_k$ is the kth concentration ratio and $\boldsymbol{\Pi} = \mathbf{C}^{-1}\mathbf{C}_0$ $(K \times K)$ is the diagonal matrix of concentration ratios. Some of the π_k are zero if the prediction sample contains components which are not present in the calibration sample. From (19) it is clear that the matrix of concentration ratios can be written as

$$\boldsymbol{\Pi} = \mathbf{X}^{+}\mathbf{R}_0\mathbf{Y}^{+\mathrm{T}} \tag{20}$$

Consequently, the kth concentration ratio is given by

* The symbol $\mathbf{R}_0$ has been used in the previous section. However, its meaning should be clear from the context.

$$\pi_k = \mathbf{x}_k^{+\mathrm{T}} \mathbf{R}_0 \mathbf{y}_k^{+} \tag{21}$$

where $\mathbf{x}_k^{+}$ $(J_1 \times 1)$ and $\mathbf{y}_k^{+}$ $(J_2 \times 1)$ are the kth row of $\mathbf{X}^{+}$ and $\mathbf{Y}^{+}$ respectively (both are column vectors).

Equation (21) can be seen as the 'model-building step'. The irony is that in this model-building step a random variable (π_k) rather than a model parameter is determined. In the 'prediction step', π_k is combined with the calibration sample concentration to obtain a prediction of the analyte concentration. Quantitation is based on the estimate for π_k. Thus the question of deriving an expression for the net analyte response matrix is equivalent to the question which part of $\mathbf{R}_0$ contributes to π_k in equation (21). This question is easily answered by expanding $\mathbf{R}_0$ in orthogonal terms as

$$\mathbf{R}_0 = \pi_k \mathbf{x}_k^{*} \mathbf{y}_k^{*\mathrm{T}} + \pi_k \mathbf{x}_k^{*} \mathbf{y}_k^{\perp\mathrm{T}} + \pi_k \mathbf{x}_k^{\perp} \mathbf{y}_k^{*\mathrm{T}} + \pi_k \mathbf{x}_k^{\perp} \mathbf{y}_k^{\perp\mathrm{T}} + \sum_{k' \neq k}^{K} \pi_{k'} \mathbf{x}_{k'} \mathbf{y}_{k'}^{\mathrm{T}} \tag{22}$$

where $\mathbf{x}_k^{*}$ $(J_1 \times 1)$ and $\mathbf{y}_k^{*}$ $(J_2 \times 1)$ are the net contributions to $\mathbf{x}_k$ and $\mathbf{y}_k$ respectively, $\mathbf{x}_k^{\perp} = \mathbf{x}_k - \mathbf{x}_k^{*}$ and $\mathbf{y}_k^{\perp} = \mathbf{y}_k - \mathbf{y}_k^{*}$. Inserting (22) in (21) shows that only the first term contributes to π_k, i.e. it is the part of the response matrix that is useful for quantitation and hence according to our definition constitutes the matrix of net partial responses. Consequently,

$$\mathbf{R}_{k,0}^{*} = \pi_k \mathbf{x}_k^{*} \mathbf{y}_k^{*\mathrm{T}} \tag{23}$$

where $\mathbf{R}_{k,0}^{*}$ $(J_1 \times J_2)$ denotes the kth net contribution to $\mathbf{R}_0$. This result does not come entirely unexpectedly. The gross response matrix is bilinear and the same is found for the net response matrix: it is bilinear in the net analyte contributions to the individual modes. Analogous to equation (10), these are given by

$$\mathbf{x}_k^{*} = (\mathbf{I}_{J_1} - \mathbf{X}_{-k} \mathbf{X}_{-k}^{+}) \mathbf{x}_k = \mathbf{P}_{k,\mathbf{X}} \mathbf{x}_k \tag{24a}$$

$$\mathbf{y}_k^{*} = (\mathbf{I}_{J_2} - \mathbf{Y}_{-k} \mathbf{Y}_{-k}^{+}) \mathbf{y}_k = \mathbf{P}_{k,\mathbf{Y}} \mathbf{y}_k \tag{24b}$$

In the following, focus is on the prediction sample response matrix (recall that some figures of merit are sample-dependent). The equations are completely analogous for the calibration sample. Combination of equations (18) and (24) and using the symmetry of $\mathbf{P}_{k,\mathbf{Y}}$ shows that the prediction sample net response matrix is given by

$$\mathbf{R}_k^{*} = \mathbf{P}_{k,\mathbf{X}} \mathbf{R} \mathbf{P}_{k,\mathbf{Y}} \tag{25}$$

The similarity to the first-order case is increased by 'stringing' out $\mathbf{R}_k^{*}$ and $\mathbf{R}$ columnwise from left to right using the vec operator (see Appendix II) and using equation (68). The result is

$$\mathrm{vec}\mathbf{R}_k^{*} = (\mathbf{P}_{k,\mathbf{Y}} \otimes \mathbf{P}_{k,\mathbf{X}})\, \mathrm{vec}\mathbf{R} = \mathbf{P}_k\, \mathrm{vec}\mathbf{R} \tag{26}$$

where $\otimes$ denotes the Kronecker product (see Appendix II). The analogues of equations (11)–(17) are now easily obtained.

'Net partial sensitivities':

$$\mathrm{vec}\mathbf{S}_k^{*} = \mathrm{vec}\mathbf{R}_k^{*} / c_k \tag{27}$$

Net analyte signal:

$$r_k^{*} = \| \mathrm{vec}\mathbf{R}_k^{*} \| \tag{28}$$

Sensitivity:

$$s_k = \| \mathrm{vec}\mathbf{S}_k^{*} \| = r_k^{*} / c_k \tag{29}$$

Relation with the 'inverse sensitivity' from the 'inverse' model:

$$s_k = \beta_k^{-1} = \| \mathbf{\beta}_k \|^{-1} = \| \mathbf{\beta}_{k,\mathbf{Y}} \otimes \mathbf{\beta}_{k,\mathbf{X}} \|^{-1} \tag{30}$$

where $\mathbf{\beta}_{k,\mathbf{X}} = c_k^{1/2}\mathbf{x}_k^+$ $(J_1 \times 1)$ and $\mathbf{\beta}_{k,\mathbf{Y}} = c_k^{1/2}\mathbf{y}_k^+$ $(J_2 \times 1)$ are 'regression vectors' in the X- and Y-order respectively. Note that the dimension of these regression vectors is $\sqrt{}$(concentration/response). Equation (30) is obtained by formulating an 'inverse model' for second-order data as

$$c_k = \mathbf{\beta}_{k,\mathbf{X}}^{\mathrm{T}}\, \mathbf{R}\, \mathbf{\beta}_{k,\mathbf{Y}} = (\mathbf{\beta}_{k,\mathbf{Y}} \otimes \mathbf{\beta}_{k,\mathbf{X}})^{\mathrm{T}}\, \mathrm{vec}\mathbf{R} = \mathbf{\beta}_k^{\mathrm{T}}\, \mathrm{vec}\mathbf{R} \tag{31}$$

The first part of this equation is essentially the same as equation (16) in Reference 3. Tensor algebraic considerations show that for second-order calibration *two* contravariant vectors have to be determined. These are combined in equation (31) using equation (68) to increase the similarity with the first-order case. (Note that the regression vectors for the individual modes appear in the Kronecker product in reverse order.) It is emphasized that the inverse model formulation for second-order data is actually a natural one although it is seldom encountered in the literature. This can be understood as follows. For first-order data the inverse model was introduced because it enables the solution of calibration problems where the limited prior knowledge about the interferents prohibits the use of the classical model. This 'inverse model advantage' is implied by the much stronger second-order advantage: an unknown background can be modeled effectively with (bilinear) second-order data using *one* calibration sample only. Expressions for the remaining figures of merit are as follows.

Selectivity:

$$\xi_k = r_k^* / \| \mathrm{vec}\mathbf{R}_k \| \tag{32}$$

Approximate signal-to-noise ratio (see Appendix I):

$$\rho\hat{k} = r_k^* / \sigma(\hat{r}_k^*) \approx r_k^* / \sigma_{\mathbf{R}} \tag{33}$$

where $\sigma_{\mathbf{R}}$ is the standard deviation of the measurement noise in $\mathbf{R}$.

Approximate limit of detection in signal space (see Appendix I and discussion following equation (17)):

$$L_{\mathrm{D},k} = E[\hat{r}_k^* \mid \mathrm{H_O}] + {}_{\alpha} \cdot \sigma(\hat{r}_k^* \mid \mathrm{H_O}) + k_\beta \cdot \sigma(\hat{r}_k^* \mid \mathrm{H_A}) \approx E[\hat{r}_k^* \mid \mathrm{H_O}] + (k_\alpha + k_\beta) \cdot \sigma_{\mathbf{R}} \tag{34}$$

The limit of detection for second-order data has not yet been systematically addressed in the literature. It seems that the only attempt in that direction has been undertaken by Faber *et al*.[12]

Until now it has been assumed that the prediction sample contains all substituents present in the calibration sample. This assumption is important if the 'model' is estimated using GRAM. In the simplest implementation of GRAM the prediction sample response matrix is decomposed using SVD and an eigenvalue problem is constructed. The eigenvalues give the concentration ratios and the eigenvectors constitute the transformation matrix that converts the left and right singular vectors into the physical profiles $\mathbf{X}$ and $\mathbf{Y}$. In the general case both samples may contain unique constituents and the procedure must be generalized (see Reference 14 for more details). In this paper it will be assumed throughout that the sum of the calibration and prediction sample response matrices is subjected to SVD if such a complication arises. As a result one has to replace $\sigma_{\mathbf{R}}$ by $\sqrt{2}\sigma_{\mathbf{R}}$ in equation (34) (see also Appendix I). It is noted that one also has to use a generalization in the simplest case if the analyte concentration approaches the limit of detection, since under those circumstances decomposing the prediction sample response matrix will not lead to stable concentration estimates. These complications are not encountered if the model is estimated using an ALS method.

It is important to note that the large majority of research in higher-order calibration methodology is concerned with the general case where multiple calibration samples are available.[28–32] The reason for this is that multiple calibration samples allow for the calculation of diagnostics, e.g. spectral residuals,

that enable the detection of outliers. This is obviously not possible in the one-calibration-sample case where the prediction sample responses are used to construct the 'model'. The one-calibration-sample case is treated extensively in this paper because it allows for a straightforward derivation of expressions, which can then often be generalized to more complex cases.

Comparison of different definitions of second-order net analyte signal

In the previous section an expression was derived for second-order net analyte signal which can be show to be consistent with the uniqueness of Ho *et al*.[10] Since the definitive priority for the *concept* of a second-order net analyte signal appears to go to Ho *et al*., this expression will therefore be referred to as the HCD definition of second-order net analyte signal (after Ho, Christian and Davidson). Other definitions are given by Wang *et al*.[16] and Messick *et al*.[18] They will be referred to as WBKGT (after Wang, Borgen, Kowalski, Gu and Turecek) and MKL (after Messick, Kalivas and Lang) respectively. It is easily shown that these definitions lead to subjecting the strung-out matrix vec**R** to the following projection matrices:

$$\text{HCD:} \qquad \mathbf{P}_k = \mathbf{P}_{k,\mathbf{Y}} \otimes \mathbf{P}_{k,\mathbf{X}} \tag{35a}$$

$$\text{WBKGT:} \qquad \mathbf{P}_k = \mathbf{I}_{J_1 J_2} \tag{35b}$$

$$\text{MKL:} \qquad \mathbf{P}_k = \mathbf{P}_{k,\mathbf{R}} \tag{35c}$$

Equation (35a) has been derived in detail above. Equation (35b) is the projection that leaves vec**R** intact ($\mathbf{I}_{J_1 J_2}$ is the $J_1 J_2 \times J_1 J_2$ identity matrix). This is consistent with the reasoning of Wang *et al*. that owing to the second-order advantage, quantitation is always possible and hence the entire signal **R** is used for quantitation. Finally, the projection matrix $\mathbf{P}_{k,\mathbf{R}}$ in equation (35c) is obtained by stringing out the pure component matrices $\mathbf{R}_k$, using these vectors to construct a matrix $\mathbf{R}_{-k}$ and calculating the net responses by replacing $\mathbf{I}_J$, $\mathbf{S}_{-k}$, $\mathbf{r}-\mathbf{b}$ and $\mathbf{P}_{k,\mathbf{S}}$ in equation (10) by $\mathbf{I}_{J_1 J_2}$, $\mathbf{R}_{-k}$, vec**R** and $\mathbf{P}_{k,\mathbf{R}}$. Surprisingly, the MKL definition is found to be the most straightforward extension of Lorber's definition of net analyte signal. For example, Figure 3 completely describes the MKL projection whereas the HCD definition essentially consists of two projections.

Table 1 summarizes the properties of the second-order selectivities calculated according to the different definitions. The selectivity is chosen because it is bounded between zero (no selectivity) and one (complete selectivity). This property greatly facilitate a comparison. In addition, in many papers on figures of merit, selectivity holds a special place (see e.g. Reference 18). Six different cases can be

Table 1. Second-order selectivity, calculated according to various definitions, as a function of the first-order selectivities

	First-order selectivity[a]		Second-order selectivity		
Case	X-order	Y-order	HCD	WBKGT	MKL
1	1	1	1	1	1
2	1	$\xi_{\mathbf{Y}}$	$\xi_{\mathbf{Y}}$	1	1
3	1	0	0	0	1
4	$\xi_{\mathbf{X}}$	$\xi_{\mathbf{Y}}$	$\xi_{\mathbf{X}} \cdot \xi_{\mathbf{Y}}$	1	$> \xi_{\mathbf{X}}$
5	$\xi_{\mathbf{X}}$	0	0	0	$\xi_{\mathbf{X}}$
6	0	0	0	0	0

[a] The data matrix is organized in such a way that the first order (X) has the highest selectivity, i.e. $1 > \xi_{\mathbf{X}} \geqslant \xi_{\mathbf{Y}} > 0$.

distinguished, depending on the values of the individual first-order selectivities. The second-order HCD selectivity is the product of the individual first-order values. This property follows directly from the bilinear structure of the net response matrix and is already reported for the equivalent uniqueness.[10] The second-order WBKGT selectivity can only take the values zero (if one of the individual values is zero) and one (otherwise). Finally, the MKL selectivity is always as good as or better than either of the individual values.[18]

The coexistence of several definitions leads to a troublesome situation (which one is correct?). Since to the authors' best knowledge no obvious relations exist between the different definitions and the apparent lack of order in Table 1 indicates that establishing a simple relationship will be extremely difficult, a choice must be made. Here it is proposed to draw upon a connection with the eigenvalues obtained from principal component analysis (PCA) or, equivalently, the singular values obtained from singular value decomposition (SVD) to show that equation (35a) gives the 'correct' definition. This connection is given by the rationale behind rank annihilation factor analysis (RAFA).

In the simplest formulation of RAFA a constant times a pure component matrix is subtracted from the prediction sample response matrix and the behavior of the last significant eigenvalue of the difference matrix is monitored as a function of that constant. It is readily seen that if the constant equals the concentration ratio $c_k/c_{k,0}$, the contribution of the kth component to the prediction sample is 'annihilated'. The annihilation of the analyte of interest leads to a minimum for the last significant eigenvalue. As an illustrative example the results of an RAFA calculation on experimental data reported by McCue and Malinowski[33] are given in Figure 4. The last significant eigenvalue does not become zero; it takes the value of the first non-significant eigenvalue, which is non-zero because it describes error variance.

Now consider a situation where the response matrices are noise-free. In the absence of noise the last significant eigenvalue describes the variance of the net analyte response matrix, i.e. it becomes identical to the squared (scalar) net analyte signal, in the limit where the analyte is annihilated.[10] This

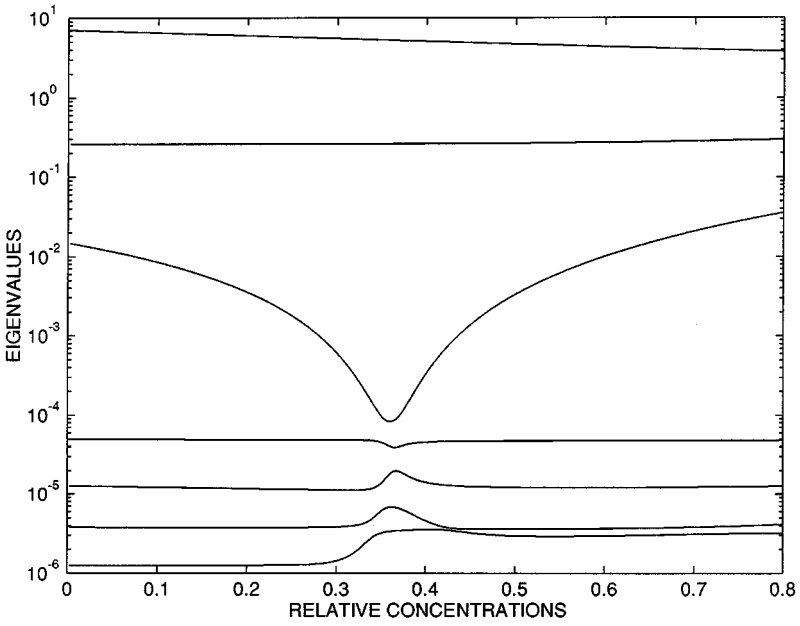

Figure 4. Eigenvalues versus relative concentrations for RAFA analysis of LC–UV data of McCue and Malinowski[33]

follows from the orthogonality of principal components and the fact that the analyte and the last significant eigenvalue are annihilated simultaneously. As a result

$$\lim_{\Delta_k \to 0} r_k^* = \sqrt{\lambda_K} = \theta_K \tag{36}$$

where Δ_k denotes the analyte concentration that appears to contribute to the difference matrix; λ_K and θ_K are the Kth eigenvalue and Kth singular value respectively. This relationship provides a simple test for the validity of the proposed definition for second-order net analyte signal: compare the (scalar) net analyte signal of a diluted component with the last singular value in a noise-free situation. Unless otherwise mentioned, the second-order figures of merit will be assumed to be derived from the HCD definition in the remainder of the paper.

Extension to the 'non-bilinear' model ('mixed complexity' data)

In the chemometrics literature a distinction is made between bilinear and so-called non-bilinear data. The data are considered to be bilinear if a (spectrally active) one-component sample gives rise to a rank-one response matrix and 'non-bilinear' otherwise. Kiers and Smilde[34] correctly point out that in a mathematical sense 'non-bilinear' data are also bilinear because they can be expanded in bilinear terms. For this type of data a one-component response matrix is given by

$$\mathbf{R}_k = \sum_{l=1}^{L_k} \mathbf{x}_{l,k} \mathbf{y}_{l,k}^{\mathrm{T}} \tag{37}$$

They prefer the psychometrics nomenclature and use the terms 'complexity-one' and 'mixed complexity' to differentiate between the cases. The preceding sections were concerned with the complexity-one case.

The extension to mixed complexity data is straightforward. The net contribution to $\mathbf{R}_k$ is obtained by constructing a projection matrix from the interferent response matrices as explained above. However, as detailed by Kiers and Smilde, data analysis for mixed complexity is severely constrained. They give a thorough account of what can be achieved with respect to extracting quantitative and qualitative information. A unique resolution of the response matrices, which is possible for complexity-one data under fairly general conditions (see next section), cannot be expected. However, for the calculation of the projection matrix it is not necessary that the interferent response matrices be resolved. Only the span of the interferent response matrices is necessary (see Figure 3). For the same reason one does not need the complete resolution of the analyte response matrix, given by equation (37), but only the sum of the individual contributions. In the remainder of the paper, complexity-one data are assumed for simplicity.

Extension to higher-order data ($N > 2$)

The extension to Nth-order data ($N > 2$) becomes obvious by applying the vec operator to equation (18) and using (69), resulting in $\mathrm{vec}\mathbf{R} = \Sigma \mathbf{y}_k \otimes \mathbf{x}_k$. Completely analogously the strung-out Nth-order tensor $\mathrm{vec}\underline{\mathbf{R}}$ with factor matrices $\mathbf{A}_n$ ($n = 1, \ldots, N$), instead of $\mathbf{Y}$ and $\mathbf{X}$, and profiles $\mathbf{a}_{k,n}$ ($k = 1, \ldots, K$ and $n = 1, \ldots, N$), instead of $\mathbf{y}_k$ and $\mathbf{x}_k$ ($k = 1, \ldots, K$) can be described as[35, 36]

$$\mathrm{vec}\underline{\mathbf{R}} = \sum_{k=1}^{K} \bigotimes_{n=1}^{N} \mathbf{a}_{k,n} \tag{38}$$

Table 2. Overview of important expressions for varying data complexity. The symbols are explained in the text

	Zeroth-order	First-order	Nth-order ($N \geqslant 2$)
Classical model	$r^* = sc$	$r_k^* = s_k c_k$	$r_k^* = s_k c_k$
Inverse model	$c = \beta r^*$	$c_k = \beta_k r_k^*$	$c_k = \beta_k r_k^*$
'Net partial responses'	$r^* = r - b$	$\mathbf{r}_k^* = \mathbf{P}_{k,s}(\mathbf{r} - \mathbf{b})$	$\mathrm{vec}\underline{\mathbf{R}}_k^* = (\bigotimes_{n=1}^{N} \mathbf{P}_{k,n})\ \mathrm{vec}\underline{\mathbf{R}}$
Net analyte signal	r^*	$r_k^* = \|\mathbf{r}_k^*\|$	$r_k^* = \|\ \mathrm{vec}\underline{\mathbf{R}}_k^*\|$
'Net partial sensitivities'	$s^* = r^*/c$	$\mathbf{s}_k^* = \mathbf{r}_k^* / c_k$	$\mathrm{vec}\underline{\mathbf{S}}^*_k = \mathrm{vec}\underline{\mathbf{R}}_k^*/c_k$
Sensitivity	s	$s_k = \|\mathbf{s}_k^*\|$	$s_k = \|\mathrm{vec}\underline{\mathbf{S}}_k^*\|$
Inverse sensitivity	β	$\beta_k = \|\boldsymbol{\beta}_k\|$	$\beta_k = \|\bigotimes_{n=1}^{N} \boldsymbol{\beta}_{k,n}\|$
Selectivity	$\xi = r^*\ /\ r$	$\xi_k = r_k^*/\|\mathbf{r}_k\|$	$\xi_k = r_k^*/\|\mathrm{vec}\ \underline{\mathbf{R}}_k\|$
Signal-to-noise ratio	$\rho = r^*/\sigma_{r-b}$	$\rho_k \approx r_k^*/\sigma_{\mathbf{r}-\mathbf{b}}$	$\rho_k \approx r_k^*/\sigma_{\mathbf{R}}$
Limit of detection	$L_D \approx (k_\alpha + k_\beta) \cdot \sigma_{r-b}$	$L_{D,k} \approx E[\hat{r}_k^* \mid H_O] + (k_\alpha + k_\beta) \cdot \sigma_{\mathbf{r}-\mathbf{b}}$	$L_{D,k} \approx E[\hat{r}_k^* \mid H_O] + (k_\alpha + k_\beta) \cdot \sigma_{\underline{\mathbf{R}}}$

where $\otimes$ denotes the N-fold Kronecker product. The analogue of equation (26) is

$$\mathrm{vec}\underline{\mathbf{R}}_k^* = \left(\bigotimes_{n=1}^{N} \mathbf{P}_{k,n}\right) \mathrm{vec}\underline{\mathbf{R}} = \mathbf{P}_k\ \mathrm{vec}\underline{\mathbf{R}} \tag{39}$$

All figures of merit now follow by simple substitutions. Table 2 gives an overview of the expressions that are obtained. There is a natural progression going from left to right in Table 2. The first-order advantage (over zeroth-order calibration) is symbolized by the presence of the analyte index k: multicomponent analysis is possible using first-order data. One allows for overlap between analyte and interferents that are included in the model. Some expressions, which are exact for zeroth-order calibration, become approximate, because the net analyte signal is obtained by projection and the projection matrix itself must be estimated. The second-order advantage can be recognized from the subscript of the response error, $\sigma_{\underline{\mathbf{R}}}$: no background correction is necessary to obtain correct concentration estimates.

Leurgans *et al.*[37] sketch a proof that the uniqueness of the resolution of Nth-order multilinear data ($N > 2$) is governed by the same conditions as the uniqueness of the resolution of bilinear data. Translated to the notation in this paper, sufficient conditions for the unique resolution of (complexity-one) bilinear data are that (i) the columns of $\mathbf{X}$ and $\mathbf{Y}$ are linearly independent and (ii) no π_k are identical. Their result implies that a significant 'third-order advantage' (or beyond) cannot be found using the current approach.

To the analytical chemist it should be appealing that the model equations (classical and inverse) can be cast into a scalar representation. Compare, for example, equation (31) with its scalar counterpart in Table 2. As a result a univariate calibration graph, which is easy to interpret (see Figure 1), can indeed be constructed independent of the complexity of the data. Table 2 also contains expressions for the 'net partial responses' and 'net partial sensitivities'. These are auxiliary variables only, which are of no concern to the analytical chemist.

Finally, it is noted that in equation (38) a suitable normalization of the individual profiles is assumed. The normalization has a profound effect on the characterization of the individual modes but not on the overall figures of merit. For example, the overall selelctivity is given as the product of the N individual selectivities (recall that for second-order data, $\xi_k = \xi_{k,\mathbf{X}} \cdot \xi_{k,\mathbf{Y}}$). An equal norm for the individual profiles will be assumed here, i.e. $\|\ \mathbf{a}_{k,n}\| = \|\ \mathrm{vec}\underline{\mathbf{R}}\|^{1/N}$ ($k = 1, \ldots, K$ and $n = 1, \ldots, N$).

Prediction error variance

The true calibration sample response(s), the calibration sample concentration (often but not always) and the prediction sample response(s) are unobservable owing to measurement errors. This results in a prediction error variance for the analyte concentration. A possible relationship between the figures of merit and the prediction error variance is important because it enables the minimization of the uncertainty in the analytical result through the optimization of an analytical figure of merit.

Additional support for the HCD definition comes from the approximate expressions for prediction error variance given below. These expressions also provide motivation for using the Euclidean norm to convert vectors and matrices to scalar values. We will restrict ourselves to the expressions that are derived for the case where the model is estimated by OLS for zeroth-order and first-order data and by GRAM for second-order data. OLS is the method of choice for zeroth-order calibration, but for first-order calibration, principal component regression (PCR) and partial least squares (PLS) are popular. Variance expressions have been derived for these methods[38, 39] and the major contribution to these expressions takes a form very similar to the OLS expressions discussed below. The alternative for GRAM is the ALS method, but for this method no dependable variance expressions are known. It is noted that Appellof and Davidson[40] give an expression obtained by error propagation, but it should be regarded with caution because a rigorous evaluation was not performed.* Independently and identically distributed (i.i.d.) measurement errors are assumed. Variance expressions have been derived for more complicated error structures—the expressions given below are simplifications thereof—but they do not allow for a simple comparison (see e.g. Reference 7).

Zeroth-order calibration

The sensitivity s in equation (1) is estimated using OLS by

$$\hat{s} = (\tilde{\mathbf{c}}_0^{\mathrm{T}}\tilde{\mathbf{c}}_0)^{-1}\tilde{\mathbf{c}}_0^{\mathrm{T}}\tilde{\mathbf{r}}_0^* \tag{40}$$

where the use of experimental data is indicated by the 'tilde'.

The prediction of analyte concentration for the unknown sample proceeds according to

$$\hat{c} = \tilde{r}^*/\hat{s} \tag{41}$$

The *approximate* variance in the predicted analyte concentration is known from basic statistics:

$$V(\hat{c}) \approx s^{-2}(h_c \cdot \sigma^2_{\mathbf{r_0}-\mathbf{b}_0} + \sigma^2_{r-b}) + h_c \cdot \sigma^2_{\mathbf{c}_0} \tag{42}$$

where $h_c = c^2(\mathbf{c}_0^{\mathrm{T}}\mathbf{c}_0)^{-1}$ is the leverage of the prediction sample, $\sigma_{\mathbf{r}_0-\mathbf{b}_0} = \sqrt{(\sigma^2_{\mathbf{r}_0} + \sigma^2_{\mathbf{b}_0})}$ and $\sigma^2_{\mathbf{c}_0}$ is the error variance of the calibration concentrations. Without uncertainties in the calibration concentrations this expression is exact.[41] All errorless quantities in equation (42) have to be replaced by quantities that are available (measured/estimated/predicted).

It is seen that the squared inverse sensitivity is a multiplier for the response terms. It is often referred to as the variance factor. Kalivas and Lang[8] give a detailed discussion of the variance factor in classical first-order calibration. The role of the sensitivity in propagating response errors can be understood from Figure 1. A region in response space is mapped onto a region in concentration space ('reverse prediction'). This mapping amounts to multiplication by the inverse sensitivity and this factor has to be squared to obtain a variance.

The leverage is associated with the terms that originate from uncertainties in the calibration data.

* Note added in proof. Very recently, expressions have been derived for the variance in the parameter estimates obtained by methods related to ALS by Paatero (*Chemometrics Intell. Lab. Syst.* in press) and Linder and Sundberg (Report No. 199, Mathematical Statistics, Stockholm, 1997). A comparison with the expression given here for GRAM as well as an interpretation in terms of analytical figures of merit is a subject for further research.

The leverage (similar to the Mahalanobis distance) indicates how the unknown sample is positioned with respect to the calibration samples. An outlying sample will have a high leverage value and consequently a relatively high prediction error variance compared with samples that fall close to calibration design points. The reason for this is that the estimated calibration line is relatively more uncertain far from the origin.*

First-order calibration

The sensitivity matrix **S** in equation (8) is estimated using OLS by

$$\hat{\mathbf{S}} = (\tilde{\mathbf{R}}_0^{\mathrm{T}} - \tilde{\mathbf{B}}_0^{\mathrm{T}})\tilde{\mathbf{C}}_0(\tilde{\mathbf{C}}_0^{\mathrm{T}}\tilde{\mathbf{C}}_0)^{-1} \tag{43}$$

The prediction of the analyte concentration for the unknown sample proceeds as

$$\hat{c}_k = \hat{\mathbf{s}}_k^{+\mathrm{T}}(\tilde{\mathbf{r}} - \tilde{\mathbf{b}}) \tag{44}$$

where $\hat{\mathbf{s}}_k^+$ is the kth row of $\hat{\mathbf{S}}^+$. (Some afterthought shows that $\hat{\mathbf{s}}_k^+$ estimates the regression vector $\boldsymbol{\beta}_k$ in the inverse model.)

The *approximate* variance in the predicted analyte concentration is given by

$$V(\hat{c}_k) \approx s_k^{-2}(h_{\mathbf{c}} \cdot \sigma^2_{\mathbf{R}_0 - \mathbf{B}_0} + \sigma^2_{\mathbf{r}-\mathbf{b}}) + h_{\mathbf{c}} \cdot \sigma^2_{\mathbf{C}_0} \tag{45}$$

where $h_{\mathbf{c}} = \mathbf{c}^{\mathrm{T}}(\mathbf{C}_0^{\mathrm{T}}\mathbf{C}_0)^{-1}\mathbf{c}$ is the leverage of the prediction sample, $\sigma_{\mathbf{R}_0 - \mathbf{B}_0} = \sqrt{(\sigma^2_{\mathbf{R}_0} + \sigma^2_{\mathbf{B}_0})}$ and $\sigma^2_{\mathbf{C}_0}$ is the error variance of the calibration concentrations. Equation (45) is a simplification of an expression derived by Bauer *et al*.[7] for heteroscedastic and uncorrelated noise. This expression further simplifies if calibration is performed with K pure samples leading to a diagonal $\mathbf{C}_0$ (this is the case considered by Lorber[4]). The discussion of equation (45) is completely analogous to the discussion of equation (41). The only difference is that for first-order data the design of all concentrations (analyte and interferents) is important to obtain a small leverage.

Second-order calibration

The special one-calibration-sample case is treated first. The general multiple-calibration-sample case is discussed below. The analyte concentration for the prediction sample is predicted as

$$\hat{c}_k = \tilde{c}_{k,0}/\hat{\pi}_k \tag{46}$$

The difference with respect to the calibration and prediction phase for zeroth-order, first-order and second-order calibration (with one calibration sample) has already been detailed above. However, once all the blocks of data are combined, the order in which this proceeds is immaterial. These differences are superficial, which also becomes apparent from the following *approximate* variance in the predicted analyte concentration:

$$V(\hat{c}_k) \approx s_k^{-2}(h_c \cdot \sigma^2_{\mathbf{R}_0} + \sigma^2_{\mathbf{R}}) + h_c \cdot \sigma^2_{c_{k,0}} \tag{47}$$

where $h_c = (c_k/c_{k,0})^2$ is recognized as the second-order leverage, $\sigma^2_{\mathbf{R}_0}$ is the response error variance for the calibration sample and $\sigma^2_{c_{k,0}}$ is the error variance of the calibration concentration.

This expression is obtained by manipulating equation (36) given by Faber *et al*.[12] Faber *et al*. failed to see that a considerable simplification was possible and consequently noted that "The generalization

* This paper is mainly concerned with zero-intercept models. If the data are mean centered, similar considerations apply. In that case the leverage quantifies the distance with respect to the mean of the training samples.

of the sensitivity concept from multivariate to bilinear calibration does not seem to be straightforward". However, as for the first-order analogue, the interpretation of equation (47) is completely analogous to the zeroth-order case. Note that this expression does not contain the concentration of other constituents. Interferents contribute to the uncertainty in prediction by decreasing the net signal of the analyte and hence the sensitivity. A large overlap will result in a large prediction error variance as in first-order calibration. The possibility of quantitation in the presence of unknown interferents is clearly reflected in the expression for prediction error variance.

Equation (47) is easily adapted for multiple calibration samples by constructing a pseudo calibration sample response matrix as the sum of the individual response matrices. The leverage in that case is given as $h_c = c_k^2(\mathbf{c}_0^{\mathrm{T}}\mathbf{c}_0)^{-1}$, which increases the similarity with zeroth-order calibration (and first-order calibration using pure samples). In zeroth-order calibration, interferents are eliminated chemically (sample clean-up) and instrumentally (background correction) in order to ensure the construction of a correct model. By moving to second-order calibration, this tedious process is avoided, since the interferents are eliminated 'mathematically'.

Comparison across data orders

An important theoretical and practical question is whether there are more advantages to be obtained by going to higher data complexity than the ability to solve more complicated calibration problems. In cases where the first- and second-order advantages are not really needed to solve the calibration problem at hand, one might still opt for a more complex method if the resulting concentration estimates are more precise. Improved signal averaging is expected,[17] but obviously this is counteracted by having a non-selective signal in the additional order(s). The net signal can be much smaller than the total signal and intuitively one expects that the value of the selectivity may give an answer to the question whether the prediction error variance *decreases* or actually *increases* by going to a higher data order. Until now the selectivity has only been treated as a qualitative figure of merit in this paper. For example, the expressions for limit of detection or prediction error variance do not explicitly contain the selectivity. It is important to note that it is not sufficient to consider the selectivity alone. For example, the HCD second-order selectivity is the product of the individual first-order selectivities, which are bounded between zero and one. Thus selectivity can only *decrease* when going from first-order to second-order data and hence selectivity alone does not give enough information to select between data orders.

The following discussion may shed light on the utility of the selectivity for comparing analytical procedures based on increasing data order. Focus will be on the sensitivity, because the sensitivity is directly related to the propagation of instrument response errors (see preceding section). Throughout the discussion it is assumed that the design of the calibration set does not change; only the complexity of the instrument responses is allowed to vary.

Consider going from zeroth-order calibration with sensitivity s to first-order calibration with sensitivity s_k for the analyte of interest. The relation of selectivity ξ_k to the change in prediction error variance is established by postulating a maximum sensitivity $s_k^{\max}$ for the case where the selectivity is one, i.e. the ideal case of a fully selective signal. It follows that

$$s_k = \frac{r_k^*}{\|\mathbf{r}_k\|}\frac{\|\mathbf{r}_k\|}{c_k} = \xi_k s_k^{\max} \tag{48}$$

A maximum sensitivity for all K components jointly will be obtained if for each component one has J/K fully selective sensors, each with their zeroth-order sensitivity s, and it is easily verified that the

maximum sensitivity will be $s_k^{\max} = \sqrt{(J/K)}\, s$. It follows that

$$s_k > s \quad \text{iff} \quad \xi_k > \sqrt{K/J}) \tag{49}$$

Depending on the number of calibration samples and the design of the concentrations, an improvement in prediction error variance is obtained if that condition is fulfilled. Note that the condition can be relaxed by increasing the maximum sensitivity for the analyte of interest at the cost of determining the other analytes less precisely. (This is done by increasing the number of sensors dedicated to the analyte of interest.) The square root dependence is an instance of the law of diminishing returns. For example, a selectivity of 0·10 may counterbalance the measurement of 100 variables. On the other hand, a selectivity of 0·10 is rather low and the measurement of many more than 100 variables is routine practice using modern chromatographs or multichannel detectors. Exactly the same reasoning applies when going from first-order to second-order and in general when adding a data order.

In the preceding discussion it has been assumed that *N*th-order data are actually analyzed using an *N*th-order calibration method, i.e. the complexity of the data is retained. An interesting problem arises if the data are collapsed and analyzed using a lower-order method. A case of special importance is where second-order data are 'strung out' into vectors and analyzed using a first-order method (OLS, PCR, PLS, etc.). It is clear that the second-order advantage is lost. However, in this section, emphasis is on the precision of the predicted analyte concentration, not on the type of calibration problem at hand. In this special case the sensitivity of the strung-out data can be calculated using the MKL projection (35c). The MKL sensitivity of the 'pseudo-first-order' data is always larger than the HCD sensitivity of the original second-order data, because the selectivity is always larger (see Table 1) and the total signal is constant. This has a beneficial effect on the propagation of the response errors. However, a comparison of the leverage expressions valid for equations (45) and (47) shows that stringing out the data leads to higher leverages unless the calibration set consists of pure samples.

In summary, depending on the data, it may be beneficial to go to a first-order data analysis and equations (45) and (47) provide the necessary objective guidelines. Unfortunately, for higher-order methods ($N > 2$) no (reliable) expressions for prediction error variance exist. However, the current treatment seems to imply that collapsing the data to second-order is promising, since the sensitivity should increase and the second-order leverage has the ideal 'zeroth-order' value.

Practical evaluation of figures of merit

Only the estimation of the net analyte signal will be considered here, since this is the key ingredient of the analytical figures of merit. It has already been pointed out by Lorber[4] for the first-order case that one should avoid calculating a projection matrix for each analyte separately. Instead the estimated net analyte signal vectors for each mode, i.e. $\hat{\mathbf{a}}^*_{k,n}$ ($k = 1, \ldots, K$ and $n = 1, \ldots, N$), are most easily obtained from the corresponding row of the pseudoinverse of the estimated factor matrices, $\hat{\mathbf{A}}_n^+$ ($n = 1, \ldots, N$), i.e. $\hat{\mathbf{a}}_{k,n}^{+\mathrm{T}}$ ($k = 1, \ldots, K$ and $n = 1, \ldots, N$). It follows from the orthogonality relationships summarized by $\hat{\mathbf{A}}_n^+ \hat{\mathbf{A}}_n = \mathbf{I}_k$, the $K \times K$ identity matrix, that

$$\hat{\mathbf{a}}_{k,n}^{+\mathrm{T}} \hat{\mathbf{a}}^*_{k,n} = \hat{\mathbf{a}}_{k,n}^{+\mathrm{T}} [\hat{\mathbf{a}}_{k,n} - (\hat{\mathbf{a}}_{k,n} - \hat{\mathbf{a}}^*_{k,n})] = 1 - 0 = 1,$$

so that

$$\hat{\mathbf{a}}^*_{k,n} = \hat{\mathbf{a}}^+_{k,n} / \| \hat{\mathbf{a}}^+_{k,n} \|^2 \tag{50}$$

Table 3. Chromatographic resolution for simulated data. The symbols are explained in the text

	Situation		
Components	I (σ=2)	II (σ=5)	III (σ=20)
A–C and C–G (Δt=9)	1·13	0·45	0·11
A–G (Δt=18)	2·25	0·90	0·23

and consequently

$$\hat{r}_k^* = \| \mathrm{vec}\hat{\underline{\mathbf{R}}}_k \| = \prod_{n=1}^{N} \| \hat{\mathbf{a}}_{k,n}^* \| = \prod_{n=1}^{N} \| \hat{\mathbf{a}}_{k,n}^+ \|^{-1} \tag{51}$$

The necessary information, i.e. the estimated factor matrices, is provided by the data analysis (GRAM, ALS, etc.). As mentioned above with respect to the analysis of mixed complexity data, the uniqueness of the resolution of the response matrices of the interferents is not required in order to unambiguously determine the figures of merit for the analyte of interest.

EXPERIMENTAL

The proposed definitions of analytical figures of merit are tested and illustrated by simulations as well as data taken from the literature. For full details on the literature data sets we refer to the original work.

Second-order: simulated data

The definitions of analytical figures of merit contain errorless quantities. They can therefore only be rigorously tested using errorless data, which are most conveniently obtained by performing simulations. Adding artificial noise to these errorless data sets allows for testing of the error analysis of Appendix I. Second-order spectrochromatograms were constructed by combining simulated Gaussian-shaped chromatograms with the UV spectra for adenine (A), cytidine (C) and guanine (G) published by Zscheile *et al*.[42] The chromatographic resolution is calculated as $R=\Delta t/w=\Delta t/4\sigma$, where Δt denotes the peak separation, w is the peak width at the baseline between tangents drawn to the steepest parts of the peak and σ is the standard deviation of the peak.[43] Table 3 summarizes the different resolutions used in this work. The peak positions for adenine, cytidine and guanine are 9, 18 and 27 respectively. In order to study the relationship between the net analyte signal and the singular values obtained by SVD, the contribution of one of the components (cytidine) was systematically

Table 4. Peak heights for three-component spectrochromatograms of 'dilution' experiment

Component	IIa	IIb	IIc	IId	IIe	IIf	IIg
Adenine	1000	1000	1000	1000	1000	1000	1000
Cytidine	5	3	1	0·5	0·3	0·1	0
Guanine	1000	1000	1000	1000	1000	1000	1000

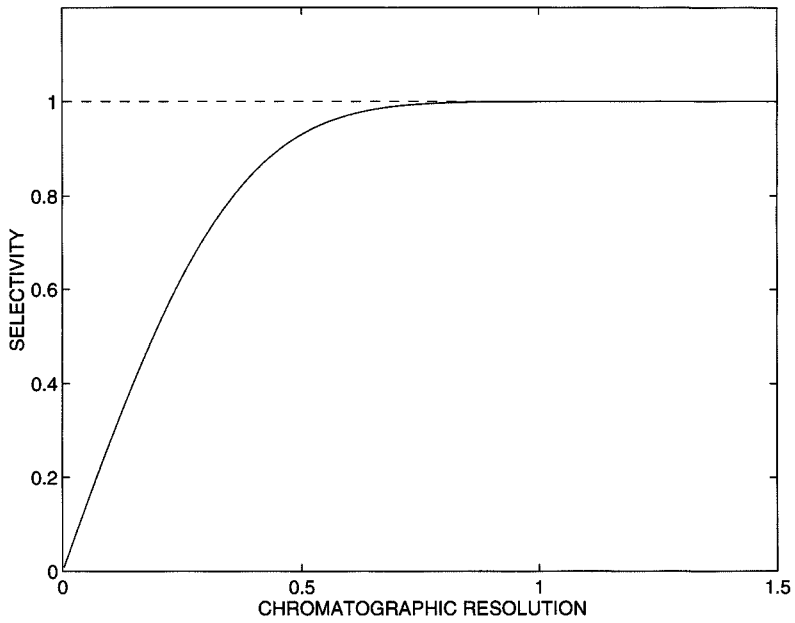

Figure 5. First-order selectivity as a function of chromatographic resolution

lowered for the middle resolution in Table 3. Table 4 describes the simulation parameters of that 'dilution' experiment. Figure 5 shows the relationship between chromatographic resolution and the associated first-order selectivity. It is seen that selectivity increases almost linearly until a resolution of 0·5 is reached, after which it levels off. Thus, in a strict mathematical sense, chromatographic resolution is not a good descriptor of selectivity. Figure 5 may be useful to interpret calculated selectivities in terms of chromatographic resolution. A response matrix consists of 36 UV spectra measured at 36 wavelengths ($J_1=J_2=36$). Figures 6 and 7 give the one-component chromatograms and spectra respectively.

First-order: near-infrared (NIR)

This data set is taken from the work of Fearn.[44] Reflectance measurements are performed at six wavelengths in the NIR region for a calibration set of 24 samples and a test set of 26 samples ($I=24$) and $J=6$). The goal of the calibration is the prediction of % protein in wheat kernels.

Second-order: liquid chromatography with ultraviolet detection (LC–UV)

This data set is taken from the work of McCue and Malinowski,[33] who described a liquid chromatograph which was especially designed for RAFA. The response matrices of mixtures of *o*-xylene, ethylbenzene and *p*-xylene were resolved using one-component response matrices (see Figure 4). Two mixtures were prepared which are denoted here as mixture I and mixture II. The concentrations of *o*-xylene, ethylbenzene and *p*-xylene in the standard solution were 1·38, 1·40 and 1·03 mg ml^{-1} respectively. A response matrix consists of seven UV spectra measured at 24 wavelengths ($J_1=7$ and $J_2=24$). Figures 8 and 9 give the one-component chromatogams and spectra respectively.

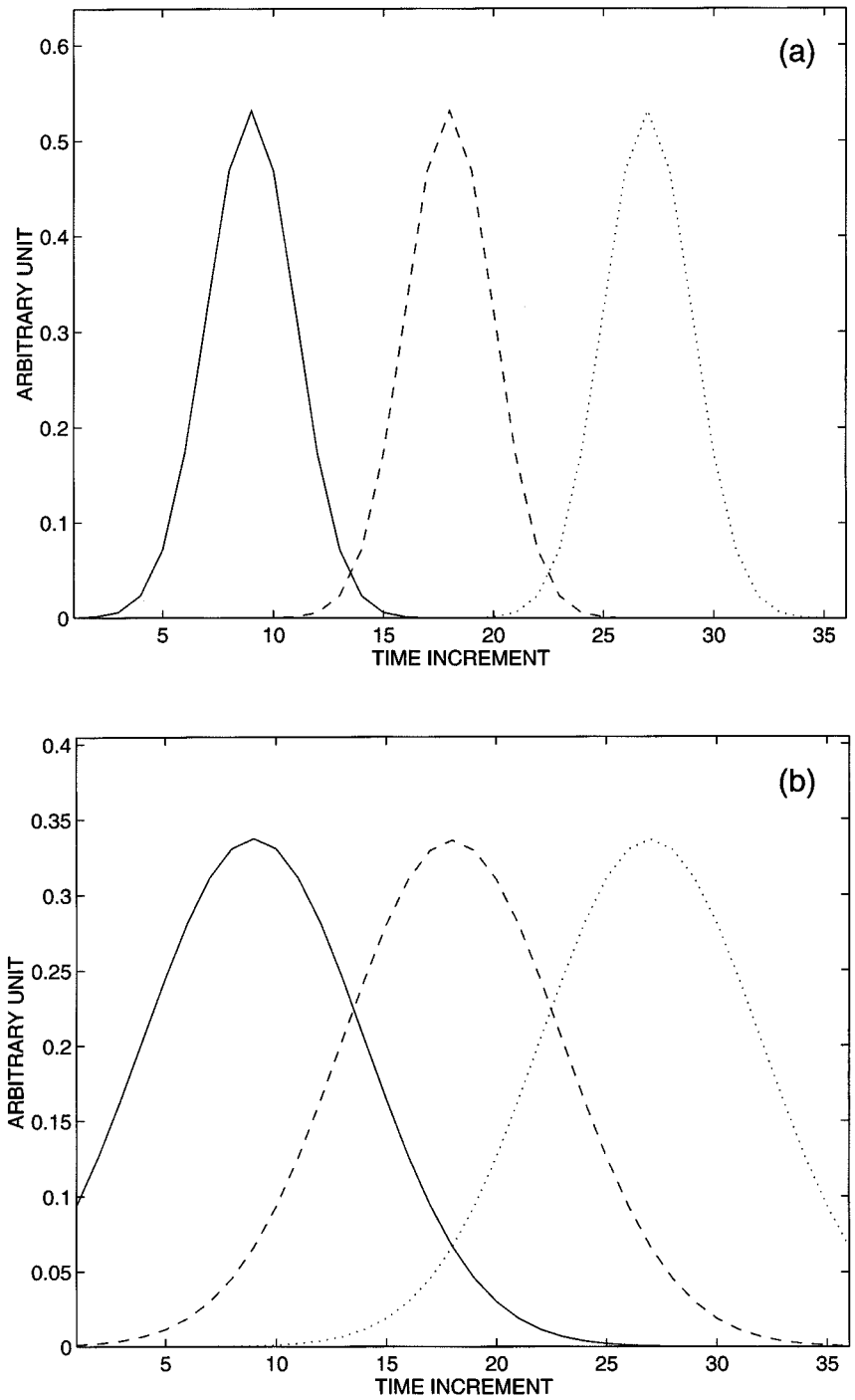

Figure 6. Normalized simulated chromatograms of adenine (——), cytidine (– – –) and guanine (· · · ·) for (a) situation I, (b) situation II and (c) situation III

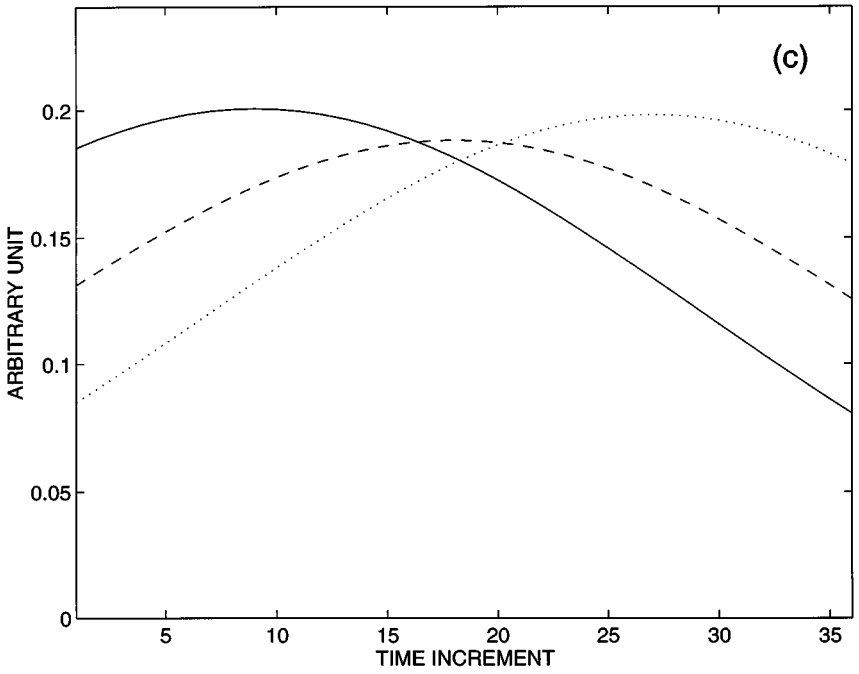

Figure 6. continued.

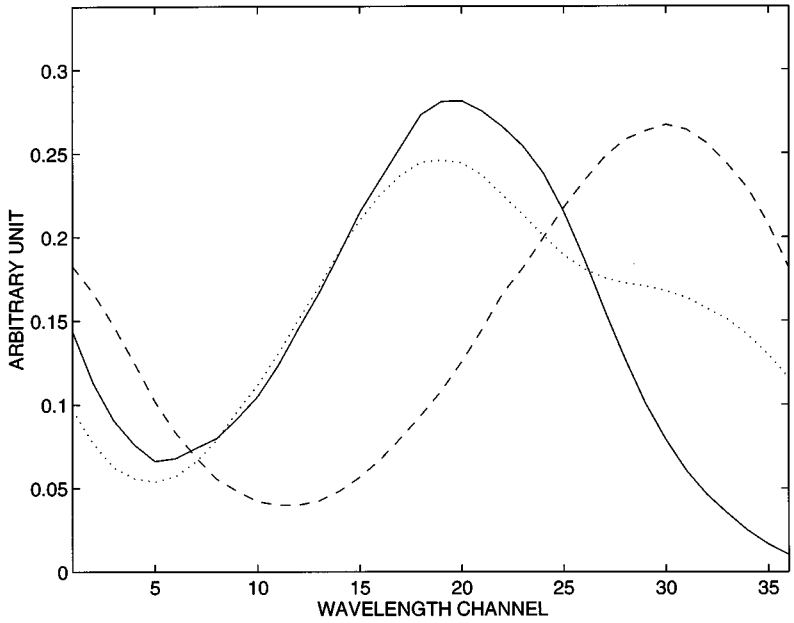

Figure 7. Normalized UV spectra of adenine (——), cytidine (– – –) and guanine (· · · ·)

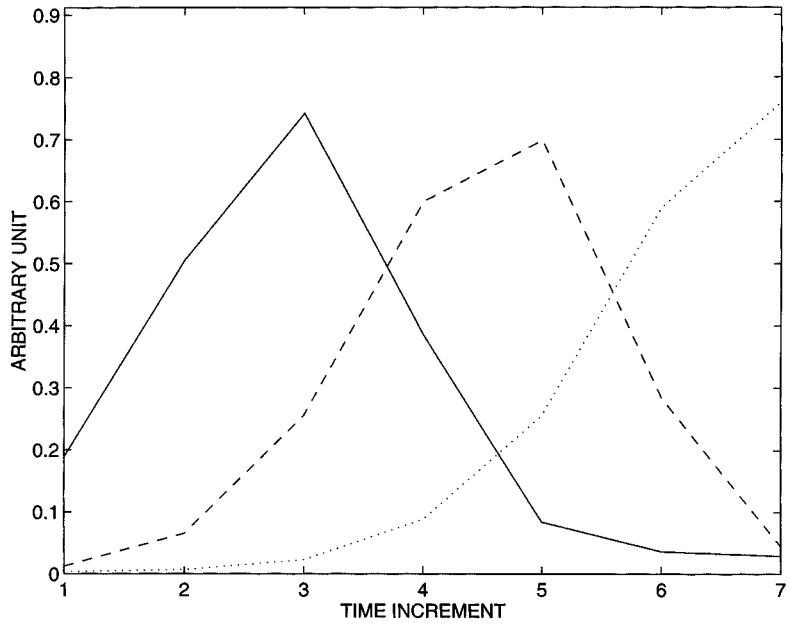

Figure 8. Normalized liquid chromatograms of ethylbenzene (——), *o*-xylene (– – –) and *p*-xylene (· · · ·)

Second-order: gas chromatography with mass spectrometry (GC–MS)

This data set is taken from the work of Colby,[45] who studied a mixture of benzene, dibromochloromethane, 1,3-dichloro-1-propene and 1,1,2-trichloroethane. The concentration in this mixture is 50 ng ml^{-1} for each analyte. The response matrix consists of 14 spectra taken at 95 masses

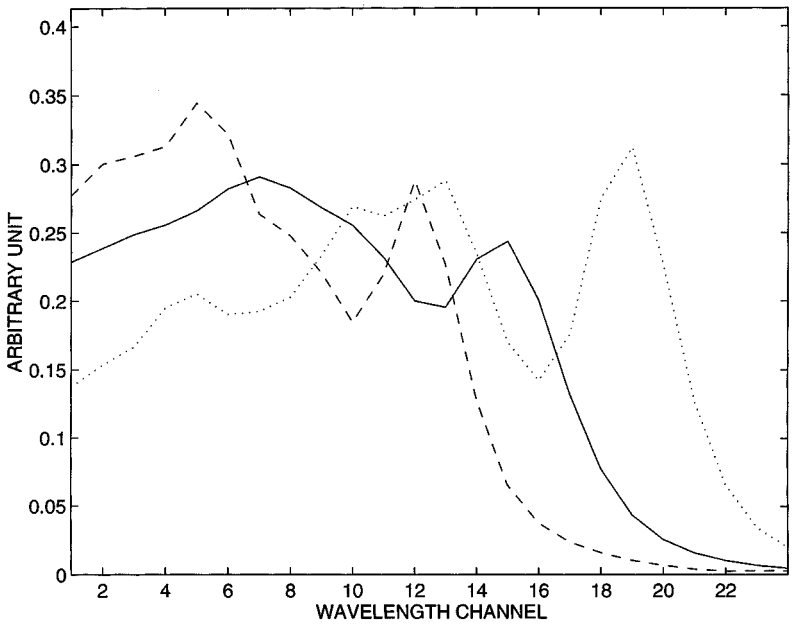

Figure 9. Normalized UV spectra of ethylbenzene (——), *o*-xylene (– – –) and *p*-xylene (· · · ·)

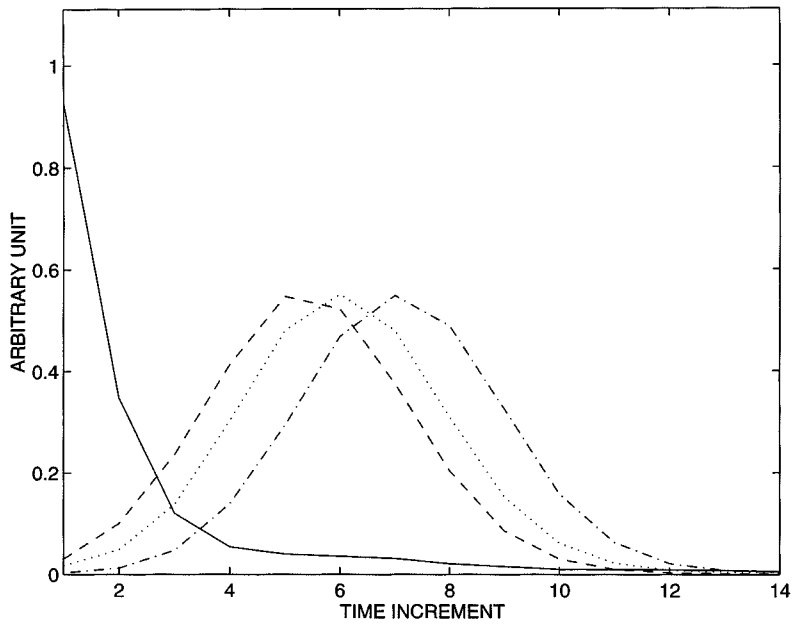

Figure 10. Normalized gas chromatograms of benzene (——), dibromochloromethane (– – –), 1,3-dichloro-1-propene (· · · ·) and 1,1,2-trichloroethane (– · –)

($J_1 = 14$ and $J_2 = 95$). Figures 10 and 11 give the one-component chromatograms and spectra respectively.

RESULTS AND DISCUSSION

Second-order: simulated data

No noise added

These simulations are performed to differentiate between the three co-existing definitions of second-order net analyte signal, summarized in equation (35).

Table 5 gives the first-order chromatographic selectivities. The very high values found for situation I are consistent with the almost baseline-resolved chromatograms observed in Figure 6(a). In this situation a conventional univariate approach can be used for quantitation. The extremely poor chromatography visible in Figure 6(c) is clearly reflected in the very low values for the selectivity. It is doubtful whether a second-order approach will work well here in the presence of realistic noise. The intermediate situation II constitutes a realistic case where a second-order approach may be successful. The chromatographic selectivity is surprisingly good: only 13%–22% loss with respect to the baseline-resolved case although the chromatographic resolution has decreased by a factor 2·5 (see Figure 5). Table 6 gives the first-order spectral selectivities. The spectral selectivities take numerical values between the chromatographic selectivities of situations II and III.

Table 7 reports the second-order selectivities calculated according to the HCD and MKL definitions. The WBKGT definition always gives the value one (see Table 1) and is therefore not included here. It is seen that the numbers in Table 7 follow the trends predicted by Table 1. The HCD selectivity is the product of the individual first-order values and the MKL selectivity is always larger than either of them. The differences are obviously largest for situation III, where the HCD values are

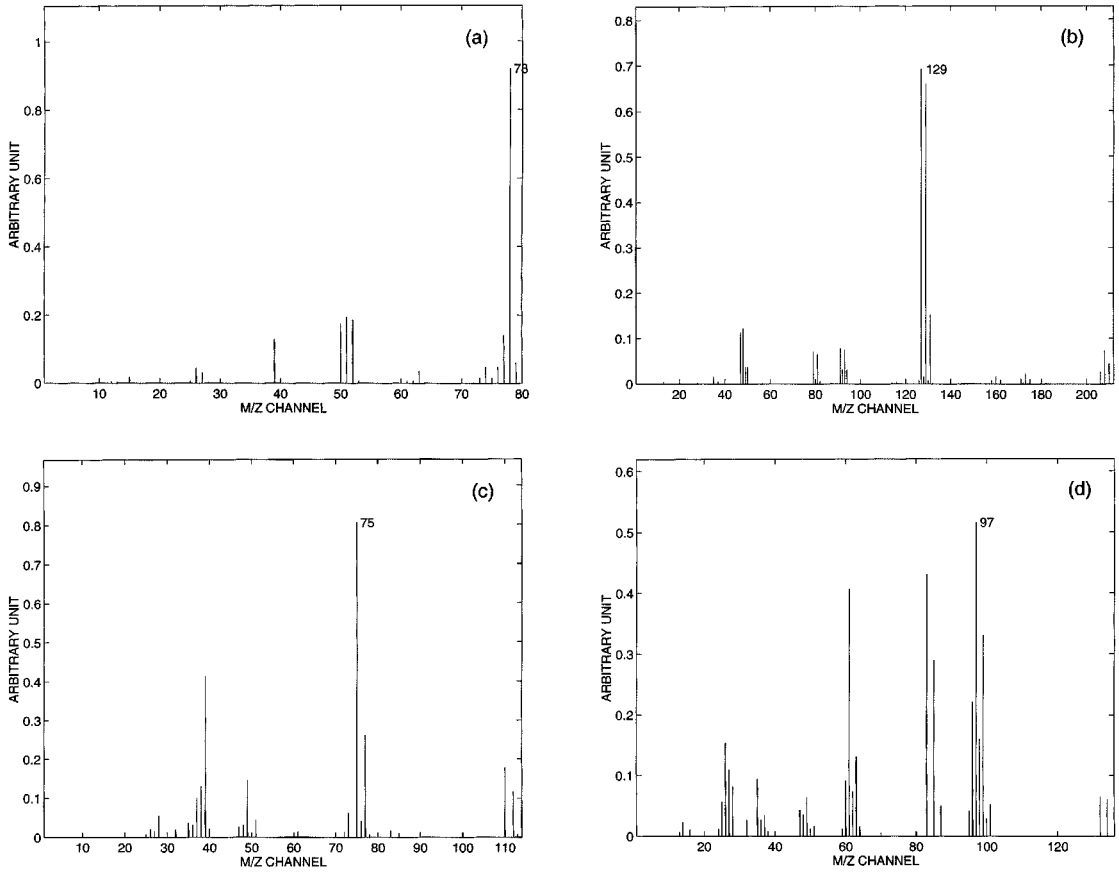

Figure 11. Normalized mass spectra of (a) benzene, (b) dibromochloromethane, (c) 1,3-dichloro-1-propene and (d) 1,1,2-trichloroethane

Table 5. First-order chromatographic selectivities for simulated data

Situation	Adenine	Cytidine	Guanine
I	0·99998	0·99996	0·99998
II	0·87680	0·78554	0·87726
III	0·04272	0·02199	0·04291

Table 6. First-order spectral selectivities for simulated data

Component	Adenine	Cytidine	Guanine
Selectivity	0·26477	0·44806	0·20055

Table 7. Second-order selectivities for simulated data

Situation	Definition	Adenine	Cytidine	Guanine
I	HCD	0·26477	0·44804	0·20054
	MKL	0·99999	0·99998	0·99999
II	HCD	0·23215	0·35197	0·17593
	MKL	0·94607	0·87777	0·92335
III	HCD	0·01131	0·00985	0·00861
	MKL	0·49194	0·56483	0·38348

extremely small and the MKL definition still leads to rather large values. For example, the MKL selectivities for adenine and guanine are almost twice as large as their spectral selectivities, which makes the interpretation of these numbers difficult in the second-order context.

Figure 12 shows the net analyte response vectors of cytidine in the chromatographic and spectral mode. The net response vectors have negative components, which is necessary to make them orthogonal with respect to the (positive) chromatograms of the interferents. Owing to the symmetry of the (simulated) chromatograms, the chromatographic net response vector is easiest to interpret. The negative lobes have their minima at 'time increments' 7 and 29, which are close to the peak maxima of adenine (9) and cytidine (27). Figure 13 gives the second-order net analyte response matrix according to the various definitions for cytidine in situation IIf. As expected, clear differences are found among these plots. For example, the projection-based definitions are distinguished by the presence of negative elements.

Table 8 summarizes the results of the 'dilution' experiment. The fourth column gives the WBKGT net analyte signal, which is equal to the (scalar) total signal. The HCD numbers in the third column are obtained by multiplying the WBKGT numbers by 0·35197, the HCD selectivity (see Table 7). Likewise the MKL numbers in the fifth column are found by multiplying the WBKGT numbers by 0·87777. The excellent agreement between the HCD numbers and the third singular value leaves no doubt about the correctness of the net analyte signal obtained from the HCD definition. Figure 14 shows the difference between the HCD net response matrix and the third singular dyad for situation IIf. Some structure is visible, but the scale of the plot makes clear that the conclusion drawn from Table 8 for the scalar net analyte signal is also valid for the net partial responses. It is emphasized that such an excellent agreement can only be demonstrated by performing simulations without noise.

Having demonstrated that the HCD definition is indeed the correct definition, the second-order selectivities in Table 7 are interpreted in terms of the expected propagation of the response errors. Combining equations (47) and (48) shows that the HCD selectivity quantifies the relative amount of error propagation in an overlapped situation compared with the fully selective case ($\xi = 1$). In this way it is found that for adenine, cytidine and guanine the variance factors are larger than the ideal values by a factor 18·6, 8·1, and 32·3 respectively. In contrast, the MKL selectivities imply that the quality of the results of a *first-order* data analysis is hardly influenced by the presence of the interferents: the smallest selectivity (for cytidine) is 0·88. The high selectivities calculated using the MKL definition are only misleading if they are applied to the original second-order data. The WBKGT definition leads to the value one for all components and therefore lacks an interpretation in terms of response error propagation.

Noise added

These simulations are performed to test the error analysis of Appendix I. Normally distributed noise with standard deviation $\sigma_{\mathbf{R}} = 0{\cdot}1$ is added (i.i.d.).

Table 9 summarizes the results of these simulations. The second column gives the true values of the net analyte signal of cytidine ($k=2$), which are obtained from the noiseless data. The predicted standard error (equation (57)) and bias (equation (63)) in the estimated net analyte signal are given in

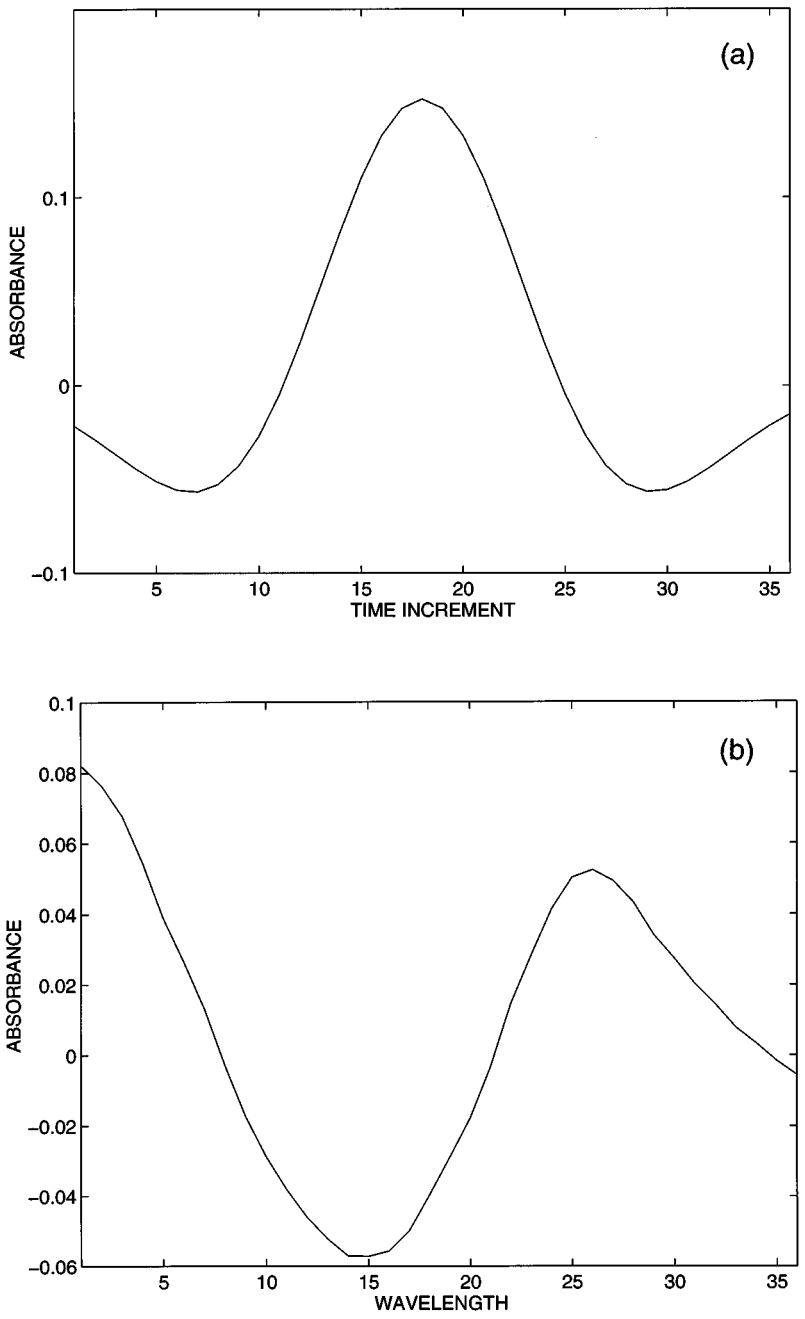

Figure 12. (a) Chromatographic and (b) spectroscopic net analyte response vector of cytidine for simulated three-component spectrochromatogram of situation IIf without noise

the next columns. These numbers have to be compared with the Monte Carlo simulation results, which are assumed to be very precise owing to the large number of replications over which they are averaged (10 000). The fifth column gives the Monte Carlo mean for the estimated net analyte signal. The next

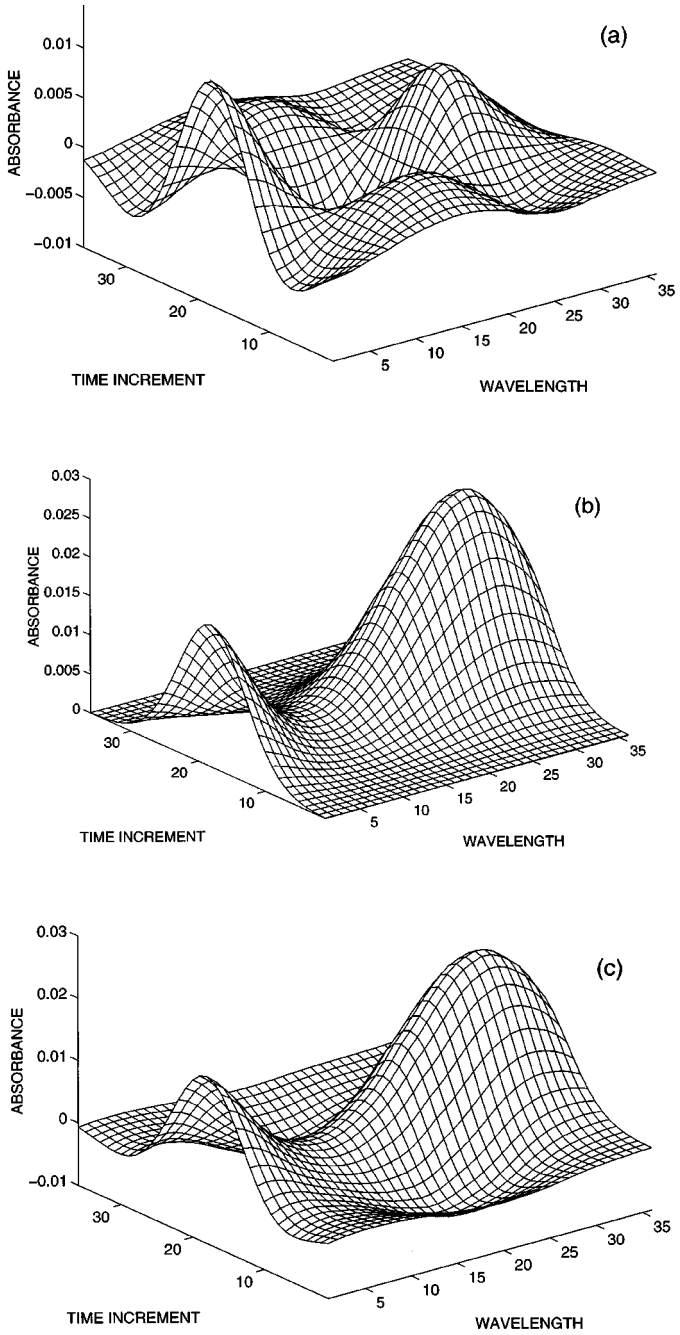

Figure 13. Net analyte response matrix of cytidine, calculated according to definition of (a) HCD, (b) WBKGT and (c) MKL, for simulated three-component spectrochromatogram of situation IIf without noise

Table 8. Comparison of second-order net analyte signal of cytidine, calculated according to various definitions, and third singular value of simulated three-component spectrochromatograms without noise

Situation	Peak height cytidine	Net analyte signal cytidine			Third singular value
		HCD	WBKGT	MKL	
IIa	5	5·2390	14·8848	13·0654	5·2299
IIb	3	3·1434	8·9309	7·8393	3·1402
IIc	1	1·0478	2·9770	2·6131	1·0474
IId	0·5	0·5239	1·4885	1·3065	0·5238
IIe	0·3	0·3143	0·8931	0·7839	0·3143
IIf	0·1	0·1048	0·2977	0·2613	0·1048
IIg	0	0	0	0	0

column gives the standard error in the estimated net analyte signal, which is calculated as the spread of the individual estimates around the mean listed in the previous column. The last column gives the bias in the estimated net analyte signal, which is calculated as the difference of the Monte Carlo mean and the true value taken from the second column. Excellent agreement is observed between the predicted standard error and bias and the Monte Carlo values for situations IIa and IIb. The agreement is good for situation IIc but poor for situation IId. This is the range where the uncertainty in the estimated net analyte signal becomes of the order of the estimate itself, i.e. one approaches the limit of detection. In this region, *qualitative* detection replaces *quantitative* determination.[22] It is seen that the standard error is always *overstimated* by equation (57). The Monte Carlo value is almost stable at situation IId. In contrast, the bias is always *underestimated* by equation (63). However, the 'true' bias increases until the net analyte signal is zero (see last column). Unfortunately, these two effects do not cancel. This is further illustrated in Figure 15, where the Monte Carlo values are bias corrected using equation (63). The difference between the bias-corrected points is larger than the predicted uncertainty for peak heights below one. It is seen that close to the limit of detection the simple error analysis of

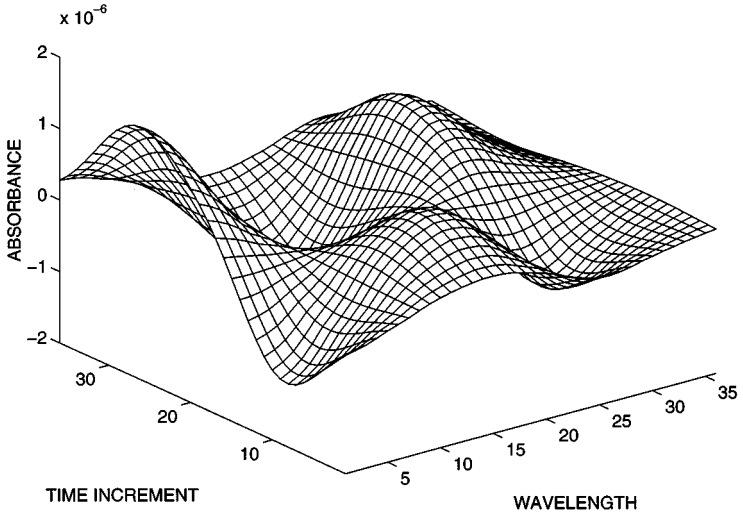

Figure 14. Difference of net analyte response matrix of cytidine, calculated according to definition of HCD, and third singular dyad for simulated three-component spectrochromatogram of situation IIf without noise

Table 9. Standard error and bias in second-order net analyte signal of cytidine, calculated according to HCD definition, for simulated three-component spectrochromatograms with noise ($\sigma_{\mathbf{R}}=0{\cdot}1$). The numbers printed in bold indicate the transition from the regime that allows for *quantitative* determination to the regime where only *qualitative* detection is possible. The symbols are defined in the text ($k=2$)

		Predicted		Monte Carlo simulations		
Situation	r_2^*	$\sigma(\hat{r}_2^*)$	$B(\hat{r}_2^*)$	$E[\hat{r}_2^*]$	$\sigma(\hat{r}_2^*)$	$B(\hat{r}_2^*)$
IIa	5·2390	0·1	0·0645	5·3029	0·1006	0·0639
IIb	3·1434	0·1	0·1064	3·2494	0·0995	0·1061
IIc	**1·0478**	**0·1**	**0·2856**	**1·3662**	**0·0839**	**0·3184**
IId	**0·5239**	**0·1**	**0·4531**	**1·1397**	**0·0488**	**0·6158**
IIe	0·3143	0·1	0·5682	1·1209	0·0452	0·8066
IIf	0·1048	0·1	0·7265	1·1153	0·0448	1·0105
IIg	0	0·1	0·8246	1·1147	0·0448	1·1147

Appendix I breaks down. For a net analyte signal (well) above the limit of detection it gives excellent results.

First-order: near-infrared (NIR)

This example is selected because calibration and prediction samples are available. This data set can therefore be used to construct a univariate calibration plot and investigate how the individual points are represented in such a plot. Furthermore, NIR spectroscopy is not used for trace analysis. For this important class of applications one will therefore not encounter the complication near the limit of detection discussed above with respect to Figure 15.

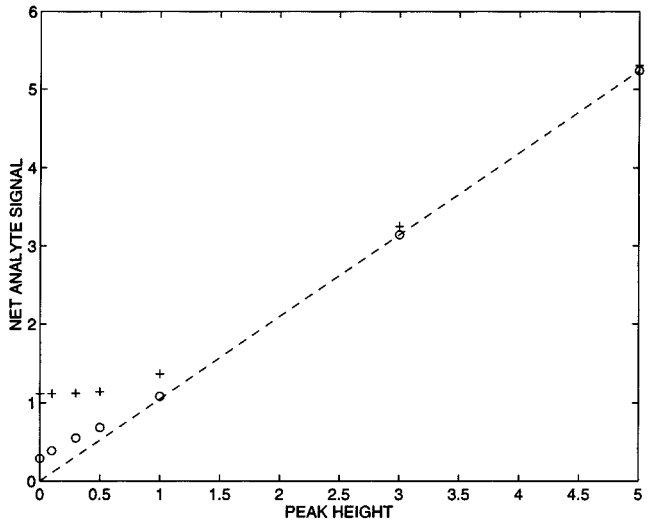

Figure 15. Monte Carlo mean before (+) and after bias correction (○) for second-order net analyte signal of cytidine, calculated according to definition of HCD, versus peak height. The broken line shows the ideal relation (no noise present)

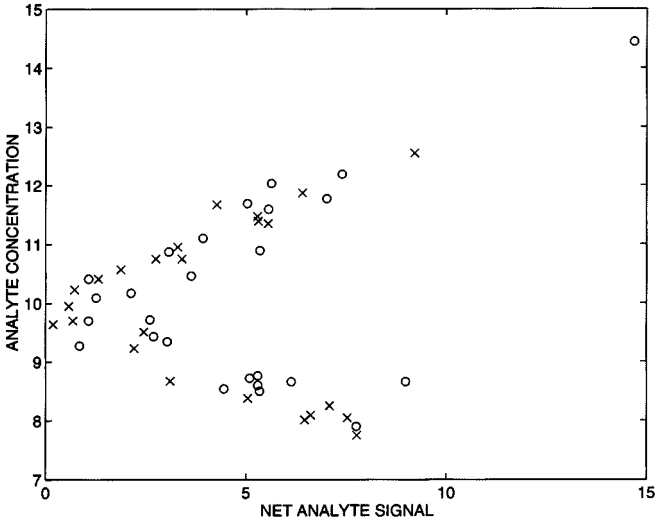

Figure 16. Analyte concentration (% protein) versus net analyte signal (NIR reflectance) without correction for mean centering for calibration (×) and prediction (○) samples

Figure 16 gives the univariate plot of analyte concentration versus net analyte signal. The projection matrix that led to the net analyte signal is based on the four-dimensional PCR model (see Reference 6 for more details). Two points are worth noting. First, the data are modeled according to the inverse model, which results in the reversal of the axes with respect to Figure 1. Second, the data are mean centered before the model is constructed. The mean centering has introduced an obvious artifact in Figure 16: the model has two 'branches'. This artifact results from converting the vector of mean-centered net responses into a scalar. Vectors that have their endpoint on equal distances 'left' and 'right' from the multivariate mean may correspond to different analyte concentrations but will be assigned the same net analyte signal value. This artifact is easily removed by undoing the centering for the net response vectors. This restores the 'natural' ordering of the points but gives abscissa values which are too high. To avoid this and at the same time obtain the desired univariate calibration graph, the points belonging to the branch with negative slope are simply reflected in the concentration axis.

It is noted that in many applications of NIR spectroscopy, optical inhomogeneities in the sample cause diffuse light scattering, which must be corrected for before the model can be built. If one uses the multiplicative scatter correction (MSC) procedure,[46] the means for all spectra are forced to be the same, so that mean centering of the data becomes almost identical with adding another principal component or PLS factor to the model. For these applications the complication just described will not occur, because mean centering is no longer necessary.

Correcting for the mean-centering artifact leads to Figure 17. The slope of the 'univariate' calibration graph is 0·285, which is the norm of the regression vector. It is emphasized that Figure 17 is not used for actual prediction but only for visualization and interpretation. For example, the residuals with respect to the calibration line are identical to the residuals calculated in the conventional way. However, being able to visualize the model leads to increased insight about the performance of the model.

In Figure 17, three points are labeled because of their high leverage in the multivariate response space. Sample 1 is an extreme outlier (leverage 6·85) and also has the largest prediction error. Samples 12 and 26 have the next two highest leverages (0·93 and 0·83). Unfortunately, this information cannot be obtained from simple inspection of Figure 17. Sample 12 is the most eccentric point in the

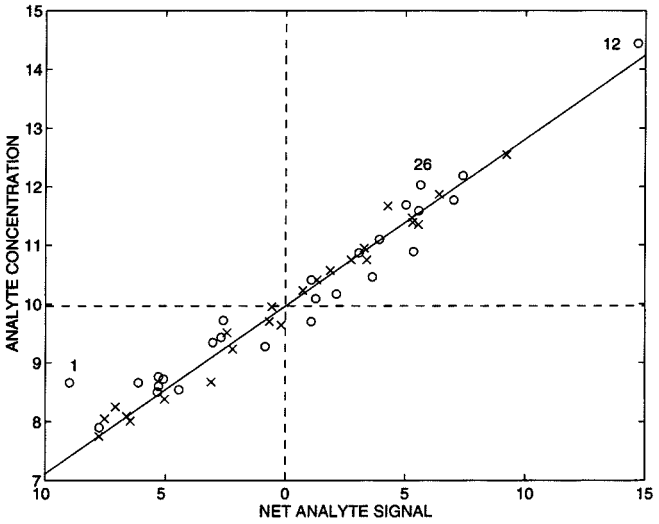

Figure 17. Analyte concentration (% protein) versus net analyte signal (NIR reflectance) after correction for mean centering for calibration (×) and prediction (○) samples. The full line is the four-dimensional PCR model and the broken lines indicate the model center

univariate sense, but sample 26, which has almost the same leverage, is well within the univariate calibration range. Sample 1 is only identified as 'special' because of its high residual. It is seen that multivariate outliers do not automatically stand out as univariate outliers. The reason is that this univariate representation of the multivariate problem is not devised to optimally preserve the topology of the multivariate space such as a non-linear mapping method would attempt to do. This can be inferred from Figure 18, where the leverage is plotted against the net analyte signal. With some imagination one may discern the desired parabola-like trend for the calibration samples, but the correlation between net analyte signal and leverage is weak. This means that, for example, adding the

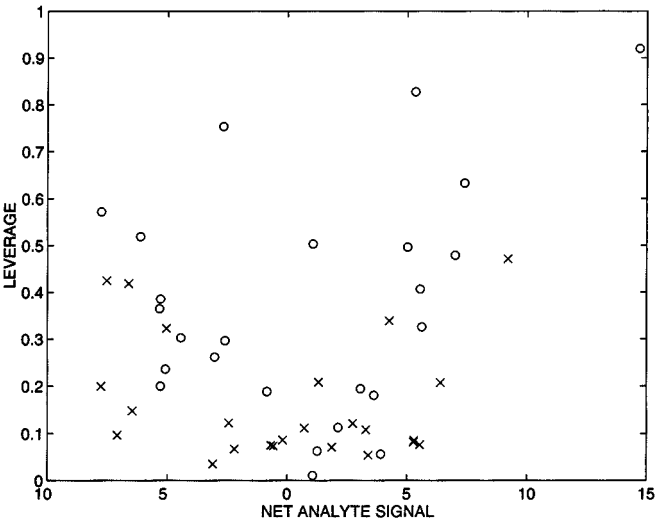

Figure 18. Leverage versus net analyte signal for calibration (×) and prediction (○) samples. Prediction sample 1 has been left out for visual clarity

Table 10. First-order selectivities for LC–UV data

Mixture	Component	LC profile	UV spectrum
I	*o*-Xylene	0·779	0·253
	Ethylbenzene	0·750	0·343
	p-Xylene	0·916	0·486
II	*o*-Xylene	0·764	0·264
	Ethylbenzene	0·743	0·321
	p-Xylene	0·900	0·457

familiar 'univariate' confidence bands to Figure 17 is not possible. However, leverage information, which is directly related to prediction error variance, can easily be added to this plot by rescaling the markers according to some function of the leverage, e.g. a sigmoid.[47]

Finally, it is noted that equation (47) suggests that the situation is simpler for second-order calibration using GRAM. In that case the univariate calibration graph can be constructed together with the confidence bands.

Second-order: liquid chromatography with ultraviolet detection (LC–UV)

McCue and Malinowski[33] measured the response matrix for two different mixtures of *o*-xylene, ethylbenzene and *p*-xylene. These mixtures only differ with respect to the weight fractions of the analytes. The weight fractions are 0·249, 0·505 and 0·247 for mixture I and 0·599, 0·203 and 0·198 for mixture II respectively. These duplicate measurements enable one to investigate the reproducibility of the analytical figures of merit which are concentration-independent, i.e. the selectivity and sensitivity. These figures of merit are model parameters rather than random variables. Table 10 gives the first-order selectivities calculated for mixtures I and II. The chromatographic and spectral selectivities are found to be reproducible within 2% and 6% respectively. This difference in reproducibility is not understood. Finally, it is seen that the chromatographic selectivities are much better than the spectroscopic selectivities. It follows that if the analytical method is to be optimized, one should try to improve the selectivity of the spectra, e.g. by a judicious choice of solvent or pH.

Table 11 lists the second-order analytical figures of merit for mixtures I and II. The net analyte signals and signal-to-noise are different for the two mixtures, since these numbers are concentration-dependent. The signal-to-noise ratio is calculated using a standard deviation of the measurement noise estimated from the residuals of a three-dimensional PCA fit of the response matrices. A value $\sigma_{\mathbf{R}} = 1$ mAU is found this way. The sensitivity and the selectivity are found to be reproducible. This means that the relationship between analyte concentration and instrumental responses is similar for both mixtures.

Table 11. Second-order analytical figures of merit for LC–UV data, calculated according to HCD definition

Mixture	Component	Net analyte signal (mAU)	Sensitivity (mAU mg^{-1} ml)	Selectivity	Signal-to-noise ratio	Limit of detection ($\mu g\ ml^{-1}$)
I	*o*-Xylene	338	325	0·197	338	9·2
	Ethylbenzene	141	282	0·257	141	10·6
	p-Xylene	662	1287	0·445	662	2·3
II	*o*-Xylene	140	334	0·202	140	9·0
	Ethylbenzene	310	254	0·238	310	11·8
	p-Xylene	495	1187	0·411	495	2·5

The last column in Table 11 gives estimates of the limit of detection expressed as analyte concentrations. Before discussing the calculation method and the significance of these numbers, it is emphasized that it is actually dubious to estimate the limit of detection from training samples with high analyte concentrations. In the current example the analyte concentrations in the standards are higher than the estimated detection limit by a factor 100 or more (see Experimental). If one realizes that most models are local approximations at best, it should be clear that any limit of detection estimate based on these data should be regarded with caution. Thus a simple approach is taken here for illustative purposes only. The numbers are obtained by approximating the limit of detection in response space as three times the standard deviation of the measurement noise (rule of thumb) and dividing this number by the second-order sensitivity, i.e.

$$\hat{L}_{\mathrm{D},k} = 3\hat{\sigma}_{\mathbf{R}}/\hat{s}_k$$

This approach amounts to neglecting the uncertainties in the calibration step.[27] It is noted that very recently Garcia *et al.*[48] have reported a successful application of this approximation in the inverse calibration setting using PLS for the determination of beta emitter (^{14}C) activity from liquid scintillation-counting data. However, a number of additional assumptions have been implicitly made. First the possibility of heteroscedasticity is ignored (see Figure 2) as well as the bias in the net analyte signal. Second, the simulations with noise added showed that theoretical error estimates, which work well at a high concentration level, tend to break down at low concentration levels (see Figure 15). This holds for the error analysis in Appendix I as well as for the prediction error variance given by equations (42), (45) and (47). Third, assumptions about response errors which may be reasonable at a high concentration level can be very unrealistic at low concentration levels. In Appendix I a symmetric distribution is assumed (characterized by one width parameter, $\sigma_{\mathbf{R}}$), whereas in practice the response error at low concentration levels is likely to follow a skewed distribution. Under the current circumstances the resulting detection limit estimates cannot be recommended for direct use. The utility of the numbers given in the last column of Table 11 primarily lies in planning the experiments that lead to dependable information from which the true limit of detection can be accurately estimated.

The foregoing gave a qualitative description of the response data. Of considerable interest in the context of the study of McCue and Malinowski is the precision of the quantitation using RAFA. The determination of ethylbenzene in mixture I is given as an example. The solutions that are injected into the chromatograph are diluted. The final estimate for the weight percentage is calculated as

$$\hat{W}_k = \hat{\tau}_k \tilde{c}_{k,0} \hat{\nu}_k / \tilde{d}$$

where $\hat{\tau}_k$ is the RAFA estimate for $c_k/c_{k,0}$, $\hat{\nu}_k$, which is determined from the dilution procedure, is the analyte concentration in the undiluted mixture divided by c_k and $\tilde{d}$ (mg ml^{-1}) is the density of the undiluted mixture (see Reference 33 for more details). The total uncertainty in the determined weight percentage is a combination of the uncertainty due to the dilution procedure and the uncertainty in the RAFA estimate. Since only products and divisions are involved, relative uncertainties in the individual contributions can be added in quadrature to obtain the desired uncertainty in the weight percentage. The total uncertainty in the dilution procedure was estimated by McCue and Malinowski to be 2·4%. Using equation (47), an uncertainty of 0·5% is found for the RAFA estimate. Combining these values (in quadrature) gives an uncertainty of 2·5% in the determined weight percentage of ethylbenzene in mixture I. This result shows that the additional uncertainty introduced by the RAFA calculation is only marginal. It confirms the conclusion of McCue and Malinowski 'that the design features, which were incorporated in the chromatograph and experimental procedure, were properly chosen and implemented'.

Second-order: gas chromatography with mass spectrometry (GC–MS)

Data obtained by mass spectrometry have the interesting feature that often fully selective channels are present, which enables a valid conventional univariate approach for calibration. A topic of practical interest is therefore to investigate how the univariate approach compares with a data analysis based on the full response matrix. In the current example, benzene, dibromochloromethane, 1,3-dichloro-1-propene and 1,1,2-trichloroethane have selective channels at $m/z = 78$, 129, 75 and 97 respectively. Apart from being selective, these channels are also very sensitive (see Figure 11), which makes the univariate approach promising. From the signal at these channels the zeroth-order figures of merit listed in Table 12 were calculated. The net analyte signal was obtained as the Euclidean norm of the chromatograms measured at the selective mass channels. Taking the Euclidean norm rather than the sum makes the numbers comparable with the second-order values. The reason for this is that the standard error in the Euclidean norm is equal to the standard deviation of the measurement noise. This is easily verified by replacing **P** by the identity matrix in equations (52)–(54) in Appendix I. The sensitivity is clearly highest for 1,3-dichloro-1-propene, followed by dibromochloromethane and 1,1,2-trichloroethane, which have similar values, and benzene, which has by far the lowest sensitivity. The signal-to-noise ratios lead to the same ranking of the analytes. These values are computed using a standard deviation of the measurement noise estimated from the residuals of a four-dimensional PCA fit of the response matrix, yielding a value $\sigma_{\mathbf{R}} = 28$. For the limit-of-detection estimates reported in the last column the same considerations hold as discussed above with respect to the LC–UV data: also for this example the actual analyte concentrations are higher than the estimated limits by two orders of magnitude.

The first-order selectivities are given in Table 13. Both chromatographic and spectral selectivities are best for benzene. The chromatographic selectivities for the remaining analytes are smaller than the spectroscopic selectivities by a factor two or more. The second-order analytical figures of merit are summarized in Table 14. A comparison with the zeroth-order values shows that only the values for benzene are slightly better, but for the remaining analytes they are clearly inferior. This can be explained in terms of the low selectivities for these analytes. For example, the selectivity for 1,3-dichloro-1-propene is only 0·046, leading to a decrease in the sensitivity and signal-to-noise ratio by a factor five. The ranking of the analytes according to their sensitivity or signal-to-noise ratio is completely changed. Benzene, which was ranked worst in the zeroth-order case, is now ranked best.

Table 12. Zeroth-order analytical figures of merit for GC–MS data

Component	Net analyte signal (ion intensity)	Sensitivity (ion intensity ng^{-1} ml)	Signal-to-noise ratio	Limit of detection (ng ml^{-1})
Benzene	13 623	272	492	0·31
Dibromochloromethane	26 352	527	951	0·16
1,3-Dichloro-1-propene	43 223	864	1560	0·10
1,1,2-Trichloroethane	24 644	493	889	0·17

Table 13. First-order selectivities for GC–MS data

Component	GC profile	Mass spectrum
Benzene	0·966	0·824
Dibromochloromethane	0·172	0·364
1,3-Dichloro-1-propene	0·117	0·388
1,1,2-Trichloroethane	0·265	0·524

Table 14. Second-order analytical figures of merit for GC–MS data, calculated according to HCD definition

Component	Net analyte signal (ion intensity)	Sensitivity (ion intensity ng^{-1} ml)	Selectivity	Signal-to-noise ratio	Limit of detection (ng ml^{-1})
Benzene	14 749	295	0·796	532	0·28
Dibromomochloromethane	8065	161	0·063	291	0·52
1,3-Dichloro-1-propene	8190	164	0·046	296	0·51
1,1,2-Trichloroethane	13 356	267	0·139	482	0·31

Based on equations (39) and (44), it is expected that the quantitation of benzene may improve (by a small amount) by going to second-order analysis, but for the other analytes a univariate calibration using selective channels is recommended.

It is noted that for this example the 'comparison across data orders' using equation (46) is not possible, because the data are not constructed according to the rigid assumption that each analyte is allotted the same number of variables (in both orders). This is immediately apparent from Figure 10, which shows that the chromatogram of benzene is truncated. The truncated chromatogram leads to a first-order selectivity of 0·966. It is clear that only a marginal improvement in this number is possible, simply because the selectivity is bounded above by one. However, this does not hold for the sensitivity, which could have been markedly improved by collecting the entire chromatogram. As a result one needs for benzene a second-order selectivity of 0·796 to only slightly improve the zeroth-order sensitivity. Equation (46) predicts the much smaller value $\xi > \sqrt{(K/J_1)} \cdot \sqrt{(K/J_2)} = \sqrt{(4 \times 4/14 \times 95)} = 0{\cdot}11$, which is not realistic under the current circumstances.

Finally, it is emphasized that this 'method comparison' can also be based on combining simulated chromatograms with library spectra, i.e. one does not have to start from a fully developed analytical technique. Evidently, these considerations should be useful in the phase of method selection. The outcome of such an analysis would likely have been that for benzene the entire chromatogram should be collected.

CONCLUSIONS

A coherent framework for analytical figures of merit for tensorial calibration has been presented. It is based on the calculation of the scalar net analyte signal as the Euclidean norm of a 'vectorized' tensor of 'partial responses'. Sensitivity (classical model), 'inverse sensitivity' (inverse model), selectivity, signal-to-noise ratio and limit of detection follow in a straightforward fashion. This allows for a completely scalar, i.e. univariate, description of an *N*th-order tensor. Consistently, this enables the presentation of an *N*th-order calibration problem as a univariate calibration graph. The possibility of characterizing *N*th-order data in the same way as univariate data is an important step in the direction of making complex data analysis techniques accessible to the practical analytical chemist.

ACKNOWLEDGEMENTS

This work was supported by the Center for Process Analytical Chemistry (CPAC), a National Science Foundation/University Cooperative Research Center at the University of Washington. Critical discussions with Peter Wentzell are appreciated by the authors. The authors are indebted to Edmund Malinowski and Bruce Colby for making their data available. Pentti Paatero and Marie Linder are thanked for sharing early versions of their work.

APPENDIX I: VARIANCE AND BIAS IN THE ESTIMATED NET ANALYTE SIGNAL

In the following derivations the subscripts are suppressed from the symbols and the background correction is left out to simplify the notation. The protection matrix **P** is assumed to be 'sufficiently' precise to neglect its contribution to the uncertainty in the estimated net analyte signal. This makes the approach independent of the estimation method and suitable for all definitions of net analyte signal discussed in this paper. The variance is derived first. We will start with the first-order case and return to the general *N*th-order case at the end.

The squared net analyte signal estimate is expressed in terms of the true (background-corrected) gross signal **r** and the measurement error d**r** as

$$(\hat{r}^*)^2 \approx (\mathbf{r} + \mathrm{d}\mathbf{r})^{\mathrm{T}}\mathbf{P}(\mathbf{r} + \mathrm{d}\mathbf{r}) \tag{52}$$

Multiplying out the right-hand side of (52) and neglecting products or error terms shows that the measurement error d**r** results in a perturbation of the squared estimate given by

$$\mathrm{d}(\hat{r}^*)^2 \approx (\mathrm{d}\mathbf{r}^{\mathrm{T}})\mathbf{P}\mathbf{r} + \mathbf{r}^{\mathrm{T}}\mathbf{P}\mathrm{d}\mathbf{r} = 2\mathbf{r}^{\mathrm{T}}\mathbf{P}\mathrm{d}\mathbf{r} \tag{53}$$

The variance in the squared estimate is given by the expected value of the squared perturbation as

$$V((\hat{r}^*)^2) = E[(\mathrm{d}(\hat{r}^*)^2)^2] = E[\mathrm{d}(\hat{r}^*)^2(\mathrm{d}(\hat{r}^*)^2)^{\mathrm{T}}] \approx 4\mathbf{r}^{\mathrm{T}}\mathbf{P}E[\mathrm{d}\mathbf{r}\mathrm{d}\mathbf{r}^{\mathrm{T}}]\mathbf{P}\mathbf{r} = 4(r^*)^2\sigma^2 \tag{54}$$

Here it has been assumed that the response errors are i.i.d. with mean zero and constant variance σ^2, i.e. $\mathbf{V}(\mathrm{d}\mathbf{r}) = E[\mathrm{d}\mathbf{r}\mathrm{d}\mathbf{r}^{\mathrm{T}}] = \sigma^2\mathbf{I}$. More complicated error models lead to an expression that contains the full covariance matrix $\mathbf{V}(\mathrm{d}\mathbf{r})$. Another expression for the variance in the squared estimate is

$$V((\hat{r}^*)^2) \approx \left(\frac{\partial(\hat{r}^*)^2}{\partial \hat{r}^*}\bigg|_{\hat{\mathbf{r}}^* = \mathbf{r}^*} \right)^2 V(\hat{r}^*) = (2r^*)^2 V(\hat{r}^*) \tag{55}$$

and combination of (54) and (55) yields

$$V(\hat{r}^*) \approx \sigma^2 \tag{56}$$

The standard error in the stimated net analyte signal follows as

$$\sigma(\hat{r}^*) \approx \sigma \tag{57}$$

Since replacing the first-order response vector by the strung-out *N*th-order tensor does not change the derivation, the result is valid in general.

The bias in the first-order net analyte signal estimate is derived as follows. First the expected value of the squared estimate is evaluated:

$$E[(\hat{r}^*)^2] \approx E[(\mathbf{r} + \mathrm{d}\mathbf{r})^{\mathrm{T}}\mathbf{P}(\mathbf{r} + \mathrm{d}\mathbf{r})] = \mathbf{r}^{\mathrm{T}}\mathbf{P}\mathbf{r} + E[(\mathrm{d}\mathbf{r}^{\mathrm{T}})\mathbf{P}\mathrm{d}\mathbf{r}] \tag{58}$$

The bias in the squared estimate is given by the difference of its expectation and the true value:

$$B((\hat{r}^*)^2) = E[(\hat{r}^*)^2] - (r^*)^2 \approx E[(\mathrm{d}\mathbf{r}^{\mathrm{T}})\mathbf{P}\mathrm{d}\mathbf{r}] \tag{59}$$

which is further manipulated to

$$B((\hat{r}^*)^2) \approx \mathrm{Tr}[E[(\mathrm{d}\mathbf{r}^{\mathrm{T}})\mathbf{P}\mathrm{d}\mathbf{r}]] = \mathrm{Tr}[E[\mathrm{d}\mathbf{r}\mathrm{d}\mathbf{r}^{\mathrm{T}}]\mathbf{P}] = \mathrm{Tr}[(\sigma^2\mathbf{I})\mathbf{P}] = (J - K + 1)\sigma^2 \tag{60}$$

where $\mathrm{Tr}[\cdot]$ denotes the trace operator. The last step follows by realizing that the trace of **P** is equal to its rank, which is easily evaluated as $J - K + 1$, since the matrix $\mathbf{S}_{-k}$ in equation (10) has only $K - 1$ independent columns. Using manipulations detailed in Reference 49, the bias in the estimated net

analyte signal follows as

$$B(\hat{r}^*) \approx \sqrt{[(r^*)^2 + (J-K)\sigma^2]} - r^* \tag{61}$$

It is important to note that the last step in equation (60) is specific for the first-order case and the final result (61) is therefore not correct in a higher-order situation. Determining the trace of **P** for higher-order data is an exercise in degrees of freedom. In general one has to take into account the order of the data as well as the estimation method. First we give the desired result for the case where bilinear data have been resolved by GRAM. The case where bilinear data have been resolved by the ALS method and the general *N*th-order case ($N>2$) are briefly discussed at the end.

When GRAM is used, the factor matrices **X** and **Y** result from rotating the singular vectors of a matrix that spans the space of all substituents in the calibration and prediction sample respectively. As a result the projection matrices associated with the factor matrices **X** and **Y** are not independent. Taking this dependence into account gives

$$B((\hat{r}^*)^2) \approx (J_1 + J_2 - K)\sigma^2 \tag{62}$$

and

$$B(\hat{r}^*) \approx \sqrt{[(r^*)^2 + (J_1 + J_2 - K - 1)\sigma^2]} - r^* \tag{63}$$

These bias expressions are identical to the bias expressions found for the eigenvalues and singular values calculated by PCA and SVD respectively.[49, 50] This result does not come as a complete surprise owing to the connection between net analyte signal and PCA (or SVD for that matter) that formed the basis for RAFA, which is equivalent to GRAM.

In the situation were the prediction sample does not span the solution space, the sum of the calibration and prediction sample matrices can be used instead. The same derivation is valid with the difference that σ^2 has to be replaced by $2\sigma^2$. This procedure will lead to a larger bias but also to a larger net analyte signal. (The same remark holds for the variance.)

The connection between RAFA and PCA leads to a simple scheme for deriving the bias in general. The term $J_1 + J_2 - K$ is the number of degrees of freedom that is 'lost' for each dimension calculated by PCA: J_1 (for the column profile) + J_2 (for the row profile) $- K$ (for the arbitrary rotation that leads to the same fit). For *N*th-order data ($N>2$) one therefore simply has to replace $J_1 + J_2 - K$ by $\sum J_n$, the number of degrees of freedom lost. (There is no arbitrary rotation.) This will also work if bilinear data have been resolved by the ALS method. In that case one combines the two response matrices into one third-order array with $J_3 = 2$ and thus obtains the factor $J_1 + J_2 + 2$.

APPENDIX II: VEC OPERATOR AND KRONECKER PRODUCT

The vec operator and the Kronecker product have a natural place in higher-order data analysis. They are often used to cast a problem in the familar matrix–vector notation. The following is a summary of useful expressions taken from Reference 35.

Let **A** be an $m \times n$ matrix and $\mathbf{a}_j$ its *j*th column; then application of the vec operator gives the $mn \times 1$ vector

$$\text{vec } \mathbf{A} = \begin{pmatrix} \mathbf{a}_1 \\ \mathbf{a}_2 \\ \vdots \\ \mathbf{a}_n \end{pmatrix} \tag{64}$$

This process is often referred to as 'stringing out' or 'vectorizing' the matrix **A**.

Let **A** be an $m \times n$ matrix and **B** a $p \times q$ matrix. The Kroncecker product of **A** and **B** is defined as the $np \times mq$ matrix given by

$$\mathbf{A} \otimes \mathbf{B} = \begin{pmatrix} A_{11}\mathbf{B} & \cdots & A_{1n}\mathbf{B} \\ \vdots & \ddots & \vdots \\ A_{m1}\mathbf{B} & \cdots & A_{mn}\mathbf{B} \end{pmatrix} \tag{65}$$

The product of two Kronecker products is given by

$$(\mathbf{A} \otimes \mathbf{B})(\mathbf{C} \otimes \mathbf{D}) = \mathbf{AB} \otimes \mathbf{CD} \tag{66}$$

if the products **AB** and **CD** exist.

The transpose of a Kronecker product is given by

$$(\mathbf{A} \otimes \mathbf{B})^{\mathrm{T}} = \mathbf{A}^{\mathrm{T}} \otimes \mathbf{B}^{\mathrm{T}} \tag{67}$$

Extremely useful is the following relation involving both the Kronecker product and the vec operator:

$$\text{vec } \mathbf{ABC} = (\mathbf{C}^{\mathrm{T}} \otimes \mathbf{A}) \text{ vec } \mathbf{B} \tag{68}$$

which holds whenever the product **ABC** is defined. Equation (68) can, for example, be used to show that for a pair of vectors **a** and **c**,

$$\text{vec } \mathbf{ac}^{\mathrm{T}} = \text{vec } \mathbf{a} \cdot 1 \cdot \mathbf{c}^{\mathrm{T}} = \mathbf{c} \otimes \mathbf{a} \tag{69}$$

For more on the vec operator and the Kronecker product see Reference 35.

REFERENCES

1. D. L. Massart, A. Dijkstra and L. Kaufman, *Evaluation and Optimization of Laboratory Methods and Analytical Procedures*, Elsevier, Amsterdam (1978).
2. E. Sánchez and B. R. Kowalski, *J. Chemometrics*, **2**, 247 (1990).
3. E. Sánchez and B. R. Kowalski, *J. Chemometrics*, **2**, 265 (1990).
4. A. Lorber, *Anal. Chem.* **58**, 1167 (1986).
5. A. Lorber, A. Harel, Z. Goldbart and I. B. Brenner, *Anal. Chem.* **59**, 1260 (1987).
6. A. Lorber, N. M. Faber and B. R. Kowalski, *Anal. Chem.* **69**, 1620 (1997).
7. G. Bauer, W. Wegscheider and H. M. Ortner, *Spectrochim. Acta*, **46B**, 1185 (1991).
8. J. H. Kalivas and P. M. Lang, *Chemometrics Intell. Lab. Syst.* **32**, 135 (1996).
9. G. Bergmann, B. von Oepen and P. Zinn, *Anal. Chem.* **59**, 2522 (1987).
10. C.-N. Ho, G. D. Christian and E. R. Davidson, *Anal. Chem.* **52**, 1071 (1980).
11. C. J. Appellof and E. R. Davidson, *Anal. Chim. Acta*, **146**, 9 (1983).
12. N. M. Faber, L. M. C. Buydens and G. Kateman, *J. Chemometrics*, **8**, 181 (1994).
13. A. Lorber and B. R. Kowalski, *J. Chemometrics*, **2**, 67 (1988).
14. E. Sánchez and B. R. Kowalski, *Anal. Chem.* **58**, 496 (1986).
15. B. E. Wilson and B. R. Kowalski, *Anal. Chem.* **61**, 2277 (1989).
16. Y. Wang, O. S. Borgen, B. R. Kowalski, M. Gu and F. Turecek, *J. Chemometrics*, **7**, 117 (1993).
17. K. S. Booksh and B. R. Kowalski, *Anal. Chem.* **66**, 782A (1994).
18. N. J. Messick, J. H. Kalivas and P. M. Lang, *Anal. Chem.* **68**, 1572 (1996).
19. B. Grung and O. M. Kvalheim, *Chemometrics Intell. Lab. Syst.* **29**, 75 (1995).
20. L. Xu and I. Schechter, *Anal. Chem.* **68**, 2392 (1996).
21. L. A. Curry, *Pure Appl. Chem.* **67**, 1699 (1995).
22. L. A. Curry, *Anal. Chem.* **40**, 586 (1968).
23. G. L. Long and J. D. Winefordner, *Anal. Chem.* **55**, 712A (1983).
24. M. Otto and W. Wegscheider, *Anal. Chim. Acta*, **180**, 445 (1986).
25. J. H. Kalivas and P. M. Lang, *Mathematical Analysis of Spectral Orthogonality*, Dekker, New York (1994).
26. G. Bauer, W. Wegscheider and H. M. Ortner, *Fresenius J. Anal. Chem.* **340**, 135 (1991).

27. R. Boqué and F. X. Rius, *Chemometrics Intell. Lab. Syst.* **32**, 11 (1996).
28. S. Wold, P. Geladi, K. Esbensen and J. Öhman, *J. Chemometrics*, **1**, 41 (1987).
29. L. Ståhle, *Chemometrics Intell. Lab. Syst.* **7**, 95 (1989).
30. P. Geladi and K. Esbensen, *J. Chemometrics*, **5**, 97 (1991).
31. A. K. Smilde and D. A. Doornbosch, *J. Chemometrics*, **6**, 11 (1992).
32. R. Bro, *J. Chemometrics*, **10**, 47 (1996).
33. M. McCue and E. R. Malinowski, *J. Chromatogr. Sci.* **21**, 229 (1983).
34. H. A. L. Kiers and A. K. Smilde, *J. Chemometrics*, **9**, 179 (1995).
35. J. R. Magnus and H. Neudecker, *Matrix Differential Calculus with Applications in Statistics and Econometrics*, Wiley, New York (1988).
36. R. Henrion, *Chemometrics Intell. Lab. Syst.* **25**, 1 (1994).
37. S. E. Leurgans, R. T. Ross and R. B. Abel, *SIAM J. Matrix Anal. Appl.* **14**, 1064 (1993).
38. A. Phatak, P. M. Reilly and A. Penlidis, *Anal. Chim. Acta*, **277**, 495 (1993).
39. N. M. Faber and B. R. Kowalski, *J. Chemometrics*, **11**, 181 (1997).
40. C. J. Appellof and E. R. Davidson, *Anal. Chem.* **53**, 2053 (1981).
41. J. C. Miller and J. N. Miller, *Statistics for Analytical Chemistry*, Ellis Horwood, New York (1993).
42. F. P. Zscheile, H. C. Murray, G. A. Baker and R. G. Peddicord, *Anal. Chem.* **61**, 2219 (1962).
43. D. C. Harris, *Quantitative Chemical Analysis*, Freeman, New York (1975).
44. T. Fearn, *Appl. Stat.* **32**, 73 (1983).
45. B. N. Colby, *J. Am. Soc. Mass Spectrom.* **3**, 558 (1992).
46. P. Geladi, D. MacDougall and H. Martens, *Appl. Spectrosc.* **39**, 491 (1985).
47. D. L. Duewer, personal communication (1996).
48. J. F. Garcia, A. Izquierdo-Ridorsa, M. Toribio and G. Rauret, *Anal. Chim. Acta*, **331**, 33 (1996).
49. N. M. Faber, M. J. Meinders, P. Geladi, M. Sjöström, L. M. C. Buydens and G. Kateman, *Anal. Chim. Acta*, **304**, 257 (1995).
50. L. A. Goodman and S. J. Haberman, *JASA*, **85**, 139 (1990).

